Revised Manuscript ID: CP-ART-05-2012-041424

Supporting Information

Some Novel Molecular Frameworks Involving Representative Elements

Arindam Chakraborty[a], Sateesh Bandaru[a], Ranjita Das[a], Soma Duley[a], Santanab Giri[b], Koushik Goswami[a], Sukanta Mondal[a], Sudip Pan[a], Soumya Sen[a] and Pratim K. Chattaraj[a,*]

[a] *Department of Chemistry and Center for Theoretical Studies*
Indian Institute of Technology, Kharagpur – 721 302, India

[b]*CIMAT, Universidad de Chile*
&
QTC, Pontificia Universidad Católica de Chile, Santiago,Chile
[*]*Corresponding author:* ***pkc@chem.iitkgp.ernet.in***

Table S1: Point group, bond length (Å) and bond angle (°) of 1,5-$C_2B_3H_5$, 1,6-$C_2B_4H_6$ and 1,7-$C_2B_5H_7$ closo carborane units optimized at M052X/6-31G(d) level of theory

Molecule	Point Group	Bond length (Å)		Bond angle (°)	
$C_2B_3H_5$	D_{3h}	C-H	1.074	<HCB	136.416
		C-B	1.554	<CBB	53.334
		B-B	1.855	<BBB	60.003
		B-H	1.180	<HBB	150.045
$C_2B_4H_6$	D_{4h}	C-H	1.075	<HCB	131.787
		C-B	1.619	<CBB	58.212
		B-B	1.706	<BBB	90.026
		B-H	1.174	<HBB	134.970
$C_2B_5H_7$	D_{5h}	C-H	1.080	<HCB	142.934
		C-B	1.730	<CBB	62.027
		B-B	1.624	<BBB	107.985
		B-H	1.080	<HBB	126.075

Table S2: Point group, bond length (Å) and bond angle (°) of single stranded polymer of 1,5-$C_2B_3H_5$, 1,6-$C_2B_4H_6$ and 1,7-$C_2B_5H_7$ closo carboranes studied at M052X/6-31G(d) level

Single stranded structures	Point Group	Bond length (Å)		Bond angle (°)	
-$C_2B_3H_3$-	D_{3h}	C-H	1.074	<HCB	136.428
		C-B	1.550	<CBB	53.565
		B-B	1.851	<BBB	59.997
		B-H	1.186	<HBB	149.996
		C-C	1.457	<BCC	136.690
-$C_2B_4H_4$-	D_{4h}	C-H	1.077	<HCB	131.725
		C-B	1.622	<CBB	58.240
		B-B	1.708	<BBB	89.995
		B-H	1.181	<HBB	135.044
		C-C	1.468	<BCC	131.881
-$C_2B_5H_5$-	C_{2h}	C-H	1.081	<HCB	126.840
		C-B	1.735	<CBB	62.008
		B-B	1.629	<BBB	107.998
		B-H	1.184	<HBB	126.013
		C-C	1.481	<BCC	127.024

Table S3: Point group, bond length (Å) and bond angle (°) of double stranded polymer of 1,5-$C_2B_3H_5$, 1,6-$C_2B_4H_6$ and 1,7-$C_2B_5H_7$ closo carboranes studied at M052X/6-31G(d) level

Double stranded structures	Point Group	Bond length (Å)		Bond angle (°)	
Helical -$C_2B_3H_3$-	D_2	C-H	1.074	<HCB	136.646
		C-B	1.551	<CBB]$_{intra}$	53.386
		B-B]$_{intra}$	1.845	<BBB	60.150
		B-B]$_{inter}$	1.684	<HBB	150.688
		B-H	1.186	<BCC	138.943
		C-C	1.456	<CBB]$_{inter}$	133.464
Linear -$C_2B_4H_4$-	D_{2h}	C-H	1.077	<HCB	131.589
		C-B	1.623	<CBB]$_{intra}$	58.334
		B-B]$_{intra}$	1.708	<BBB	90.383
		B-B]$_{inter}$	1.666	<HBB	135.095
		B-H	1.181	<BCC	131.878
		C-C	1.468	<CBB]$_{inter}$	138.386
Helical -$C_2B_5H_5$-	D_2	C-H	1.081	<HCB	126.304
		C-B	1.739	<CBB]$_{intra}$	61.511
		B-B]$_{intra}$	1.630	<BBB	107.829
		B-B]$_{inter}$	1.678	<HBB	125.892
		B-H	1.184	<BCC	130.681
		C-C	1.481	<CBB]$_{inter}$	143.110

Table S4: The total energy (E, au), electronegativity (χ, eV), hardness(η, eV) and electrophilicity (ω, eV) of 1,5-$C_2B_3H_5$, 1,6-$C_2B_4H_6$ and 1,7-$C_2B_5H_7$ closo carboranes and their single and double stranded analogues at M052X/6-31G(d) level

Molecule	E	χ	η	ω
$C_2B_3H_5$	-153.78284	4.738	10.418	1.078
$C_2B_4H_6$	-179.25755	3.857	9.948	0.748
$C_2B_5H_7$	-204.63966	4.086	9.527	0.876
Single stranded -$C_2B_3H_3$-	-1831.96934	4.090	7.816	1.070
Single stranded -$C_2B_4H_4$-	-2137.60161	4.342	9.005	1.047
Single stranded -$C_2B_5H_5$-	-2442.11988	4.304	8.809	1.051
Double stranded Helical -$C_2B_3H_3$-	-3649.84411	4.390	6.245	1.543

Double stranded Linear -$C_2B_4H_4$-	-4261.15781	4.356	7.724	1.228
Double stranded Helical -$C_2B_5H_5$-	-4870.20185	4.292	8.133	1.133

Table S5: Point group, bond length (Å) and bond angle (°) of carborane cages studied at M052X/6-311+G(d,p) level.

Molecule	Point group	Bond length (Å)		Bond angle (°)	
$(C_{12}B_6H_6)_2H_6$	D_{3h}	C-C	1.40, 1.54	<CCC	117.4, 121.9, 113.5, 111.7
		C-B	1.56, 1.60	<CCB	96.9, 98.5
		C-H	1.08, 1.10	<CCH	116.3, 120.4
		B-B	1.78	<CBC	110.5
		B-H	1.34	<BCB	85.3, 123.3
				<CBB	132.3, 114.3
				<BHB	83.6
$(C_{12}B_6H_6)_2H_{12}$	D_{6h}	C-C	1.34, 1.54	<CCC	120.0, 114.9
		C-B	1.62	<CCB	95.3
		C-H	1.09	<CCH	114.7
		B-B	1.80	<CBC	112.3
		B-H	1.35	<BCB	114.1
				<CBB	120.2
				<BHB	83.4, 87.9

Table S6: The total energy (E, au), electronegativity (χ, eV), hardness(η, eV) and electrophilicity (ω, eV) of carborane cages studied at M052X/6-311+G(d,p) level

Molecule	E	χ	η	ω
$(C_{12}B_6H_6)_2H_6$	-1223.30970	4.141	6.125	1.400
$(C_{12}B_6H_6)_2H_{12}$	-1227.07663	3.789	7.141	1.005

Table S7: The molecular point groups and the important geometrical parameters (bond lengths and inter-bond angles) of the hydrogen-bound carbon-nitrogen cages at M052X/6-31G(d,p) level.

Molecule	Point Group	Bond length (Å)		Bond angle (°)	
$C_{12}N_6$	C_{6v}	C-C	1.38, 1.51	<CCC	120
		C-N	1.32, 1.40	<CNC	102.1
				<NCN	123.7
$C_{12}N_6H_{12}$	C_{6v}	C-C	1.38, 1.51	<CCC	120
		C-N	1.47	<CNC	112.7
		C-H	1.10	<NCN	117.2
		N-H	1.01	<CCH	115.8
				<CNH	112.7
$C_{12}N_6H_{18}$	C_2	C-C	1.54, 1.59, 1.55	<CCC	119.7, 119.3, 119.7
		C-N	1.45, 1.46, 1.43, 1.44	<CNC	107.6, 112.3, 106.9
		C-H	1.09, 1.10	<NCN	114.1, 114.8, 111.5
				<CCH	108.0, 108.7, 110.3, 111.7
		N-H	1.00, 1.01	<CNH	108.9, 112.1, 109.1
				<NCH	109.1, 111.9, 109.9

Table S8: The total energy (E, au), electronegativity (χ, eV), hardness(η, eV) and electrophilicity (ω, eV) of carbon-nitrogen cages studied at M052X/6-31G(d,p) level

Moleucle	E	χ	η	ω
$C_{12}N_6$	-785.32969	5.834	5.183	3.283
$C_{12}N_6H_{12}$	-792.81451	3.417	7.482	0.780
$C_{12}N_6H_{18}$	-796.54640	1.855	9.241	0.186

Table S9: Different five membered star like clusters, their corresponding point groups, total energies (E, au) at B3LYP/6-311++G(d,p), MP2/6-311++G(d,p) and M052X/6-311++G(d,p) levels of theory and electronegativity (χ, eV), hardness (η, eV). electrophilicity (ω, eV) at B3LYP/6-311++G(d,p) level of theory.

Clusters	PG	E (B3LYP)	E (MP2)	E (M052X)	χ	η	ω
C_4OLi_5		-265.28307	-264.31007	-265.24555	2.115	3.420	0.654
Pentalithio furan	C_{2V}						
Star ($^2A_1$)		0 (78.9)	1 (115.6i)	0 (62.8)			
C_4OLi_5		-265.28306	-264.36329	-265.24555			
Pentalithio furan	C_1				2.113	3.415	0.654
Star (^2A)		0 (76.7)	0 (47.4)	0 (64.4)			
C_4NLi_5		-244.82603	-243.94655	-244.80492			
Pentalithio pyrrole	C_{2V}				2.637	4.607	0.754
star ($^1A_1$)		0 (94.0)	0 (83.0)	0 (88.4)			
C_3NOLi_5		-281.95625	-280.92982	-281.91721			
Pentalithio oxazole	C_s				2.355	2.585	1.073
star ($^1A'$)		0 (38.7)	2 (203.4i)	0 (39.5)			
C_3NOLi_5		-281.95624	-281.00776	-281.91569			
Pentalithio oxazole	C_1				2.356	2.585	1.073
star (^1A)		0(37.0)	0(29.8)	1(64.0i)			
$C_3N_2Li_5$ (1,2)		-261.51600	-260.60589	-261.47911			
Pentalithio pyrazole	C_{2v}				2.060	3.123	0.679
star ($^2A_1$)		0(92.4)	0 (76.7)	0(83.8)			
$C_3N_2Li_5$ (1,3)		-261.53937	-260.58184	-261.50207			
Pentalithio imidazole	C_{2v}				1.957	2.820	0.679
star ($^2A_1$)		0 (103.9)	1 (179.2i)	0 (93.1)			
$C_3N_2Li_5$ (1,3)		-261.53937	-260.62498	-261.50207			
Pentalithio imidazole	C_s				1.957	2.820	0.679
star ($^2A'$)		0 (104.4)	0 (76.7)	0 (93.6)			

$C_2N_3Li_5$ (1,2,3)		-278.16264	-277.13863	-278.12381			
Pentalithio-1,2,3-triazole star ($^1A_1$)	C_{2v}	0(52.3)	0(85.7)	1(33i)	2.298	2.746	0.962
$C_2N_3Li_5$ (1,2,3)		-278.16262	-277.23211	-278.12458			
Pentalithio-1,2,3-triazole star (^1A)	C_1	0(50.4)	0 (28.8)	0 (17.0)	2.297	2.747	0.961
$C_2N_3Li_5$ (1,2,4)		-278.20008	-277.26036	-278.16131			
Pentalithio-1,2,4-triazole star ($^1A'$)	C_s	0 (58.5)	0 (29.3)	1 (74.6i)	2.411	2.576	1.128
$C_2N_3Li_5$ (1,2,4)	C_1	-278.19811	-277.26607	-278.17225			
Pentalithio-1,2,4-triazole star (^1A)		0 (121.3)	0 (109.3)	0 (130.7)	2.279	3.464	0.750
C_4PLi_5		-531.42773	-530.16639	-531.39198			
Pentalithio phosphole star ($^1A_1$)	C_{2v}	0 (55.6)	1 (31.9i)	0 (60.5)	2.712	4.760	0.773
C_4PLi_5		-531.42773	-530.16640	-531.39198			
Pentalithio phosphole star ($^1A'$)	C_s	0(55.6)	0(37.8)	0 (60.5)	2.712	4.760	0.773
C_3PNLi_5 (1,2)		-548.12955	-546.78060	-548.07841			
Pentalithio-1,2- aza phosphole star ($^2A'$)	C_s	0 (10.1)	2 (136.8i)	1(43.9i)	2.218	3.504	0.702
C_3PNLi_5 (1,3)		-548.12796	-546.78509	-548.02958			
Pentalithio-1,3- aza phosphole star ($^2A'$)	C_s	0 (48.7)	2 (160.6i)	2(194.4i)	2.089	3.055	0.714
C_4SLi_5		-588.25880	-586.89782	-588.16211			
Pentalithio thiophene Star ($^2A_1$)	C_{2v}	1 (117.3i)	3 (114.1i)	3 (150i)	2.036	2.774	0.747
C_4SLi_5		-588.28082	-586.99177	-588.23880			
Pentalithio thiophene Star (^2A)	C_1	0 (87.0)	0 (78.2)	0 (79.4)	2.298	3.564	0.741

[Number of imaginary frequency (NIMAG) and ν_{min} in cm^{-1}(in bracket) is given below the total energy.]

Table S10: Different six membered star like clusters, their corresponding point groups, total energies (E, au) at B3LYP/6-311++G(d,p), MP2/6-311++G(d,p) and M052X/6-311++G(d,p) levels of theory and electronegativity (χ,eV), hardness (η, eV). electrophilicity (ω, eV) at B3LYP/6-311++G(d,p) level of theory.

Clusters	PG	E (B3LYP)	E (MP2)	E (M052X)	χ	η	ω
		-234.05493	-a-	-234.02191			
$B_3C_3Li_6$	C_s				2.010	3.075	0.657
(^{2}A')		0 (69.1)		0 (50.4)			
$B_3N_3Li_6$		-284.24255	-283.18754	-284.21065			
(Hexalithio	D_{3h}				2.398	3.708	0.775
borazine star)		0 (50.4)	0 (32.7)	0 (35.7)			
($^1A_1$')							
$B_3O_3Li_6$		-345.65259	-344.50705				
(Hexalithio	C_1			-a-	2.646	4.863	0.720
boroxine star)		0 (45.0)	0 (38.8)				
(^{1}A)							
$C_4N_2Li_6$							
(Hexalithio	C_{2V}	-307.10288	-306.01090	-307.05580			
pyridazine star)					2.175	2.671	0.886
($^1A_1$)		0 (24.3)	0 (68.1)	0 (54.1)			
$C_4N_2Li_6$							
(Hexalithio	C_{2V}	-307.13555	-306.03965	-307.08962			
pyrimidine					2.275	2.626	0.986
star) ($^1A_1$)		0 (92.9)	0 (77.1)	0 (85.7)			
$C_4N_2Li_6$							
(Hexalithio	D_{2h}	-307.09138	-306.00253	-307.05896			
pyrazine star)					2.046	1.007	2.079
(^1A_g)		2 (138.2i)	3 (247.8i)	1 (77.5i)			
$C_4N_2Li_6$			-306.02802	-307.07624	2.300	2.502	1.057
(Hexalithio	C_{2V}	-307.12553					

pyrazine star)		0 (60.3)	2 (47.1i)	
($^1A_1$)	0 (86.3)			

[Number of imaginary frequency (NIMAG) and ν_{min} in cm^{-1}(in bracket) is given below the total energy.]

Table S11: The NICS values (in ppm) of different five-membered star like clusters at B3LYP/6-311++G(d,p) level of theory.

Clusters	PG	NICS						
		0	0.5	1.0	1.5	2.0	2.5	3.0
C_4OLi_5 Pentalithio furan star	C_{2V}	-6.233	-9.296	-9.675	-6.770	-4.207	-2.626	-1.703
C_4OLi_5 Pentalithio furan star	C_1	-6.235	-9.314	-9.690	-6.777	-4.208	-2.625	-1.703
C_4NLi_5 Pentalithio pyrrole star	C_{2V}	-6.926	-10.284	-10.724	-7.430	-4.555	-2.814	-1.809
C_3NOLi_5 Pentalithio oxazole star	C_s	-11.800	-14.086	-12.987	-9.143	-6.051	-4.056	-2.783
C_3NOLi_5 Pentalithio oxazole star	C_1	-11.835	-14.528	-13.022	-9.097	-6.047	-4.077	-2.807
$C_3N_2Li_5$ Pentalithio pyrazole star	C_{2v}	-5.886	-10.768	-12.124	-8.680	-5.476	-3.436	-2.231
$C_3N_2Li_5$ Pentalithio imidazole star	C_{2v}	-6.395	-10.921	-11.950	-8.508	-5.462	-3.543	-2.371
$C_2N_3Li_5$ (1,2,3) Pentalithio-1,2,3-triazole star	C_{2v}	-12.008	-16.474	-16.274	-11.382	-7.342	-4.809	-3.253
$C_2N_3Li_5$ (1,2,3) Pentalithio-1,2,3-triazole star	C_1	-12.048	-16.889	-16.628	-11.652	-7.547	-4.956	-3.354
$C_2N_3Li_5$ (1,2,4) Pentalithio-1,2,4-triazole star	C_s	-11.904	-15.633	-15.061	-10.534	-6.896	-4.602	-3.158
$C_2N_3Li_5$ (1,2,4) Pentalithio-1,2,4-	C_1	-16.826	-15.218	-12.526	-8.016	-4.774	-2.926	-1.885

triazole star								
C_4PLi_5 Pentalithio phosphole star	C_{2v}	-11.064	-12.624	-11.872	-8.420	-5.377	-3.419	-2.233
C_3PNLi_5 (1,2) Pentalithio-1,2- aza phosphole star	C_s	-10.396	-12.674	-12.343	-8.910	-5.806	-3.735	-2.441
C_3PNLi_5 (1,3) Pentalithio-1,3- aza phosphole star	C_s	-10.042	-12.083	-12.898	-9.487	-6.270	-4.071	-2.686
C_4SLi_5 Pentalithio thiophene star	C_{2v}	-12.166	-13.565	-12.306	-8.552	-5.417	-3.433	-2.236
C_4SLi_5 Pentalithio thiophene star	C_1	-10.285	-12.849	-12.632	-8.868	-5.590	-3.522	-2.290

Table S12: The NICS values (in ppm) of different six-membered star like clusters at B3LYP/6-311++G(d,p) level of theory.

Clusters	PG	NICS						
		0	0.5	1.0	1.5	2.0	2.5	3.0
$B_3C_3Li_6$ ($^2A'$)	C_s	-27.245	-23.316	-15.790	-10.000	-6.403	-4.183	-2.814
$B_3N_3Li_6$ (Hexalithio borazine star)	D_{3h}	-0.575	-1.657	-1.983	-1.050	-0.261	-0.121	-0.254
$B_3O_3Li_6$ (Hexalithio boroxine star)	C_1	2.774	0.574	-1.197	-1.141	-0.805	-0.565	-0.410

$C_4N_2Li_6$ (Hexalithio pyridazine star) ($^1A_1$)	C_{2V}	-3.260	-7.921	-11.068	-9.092	-6.318	-4.304	-3.002
$C_4N_2Li_6$ (Hexalithio pyrimidine star) ($^1A_1$)	C_{2V}	-2.615	-7.368	-10.704	-8.939	-6.329	-4.379	-3.078
$C_4N_2Li_6$ (Hexalithio pyrazine star) ($^1A_1$)	C_{2V}	-1.293	-6.426	-10.110	-8.767	-6.391	-4.497	-3.184

Table S13: The Wiberg bond indices of various bonds (WBI_{B-X}) and the total WBI at B atom ($WBI_{B\ (Tot)}$) assessed at B3LYP/6-311+G(d) level

Clusters	Bond centers	WBI_{B-X}	$WBI_{B\ (Tot)}$
BAl_5 (D_{5h} $^1A_1'$)	B(1) – Al(2)	0.648	3.218
	B(1) – Al(3)	0.640	
	B(1) – Al(4)	0.640	
	B(1) – Al(5)	0.645	
	B(1) – Al(6)	0.645	
BAl_4Be^- (C_{2V} $^1A_1$)	B(2) – Be(1)	0.719	3.386
	B(2) – Al(3)	0.700	
	B(2) – Al(4)	0.694	
	B(2) – Al(5)	0.635	
	B(2) – Al(6)	0.638	
$LiBAl_4Be$ (C_s $^1A'$)	B(2) – Be(1)	0.819	3.384
	B(2) – Al(3)	0.659	
	B(2) – Al(4)	0.590	
	B(2) – Al(5)	0.564	
	B(2) – Al(6)	0.719	
$BAl_4Be_2^+$ (C_s $^1A'$)	B(2) – Be(1)	0.790	3.511
	B(2) – Al(3)	0.609	
	B(2) – Al(4)	0.776	
	B(2) – Al(5)	0.778	
	B(2) – Al(6)	0.341	
	B(2) – Be(1)	0.665	
	B(2) – Al(3)	0.732	

$BAl_3Be_2^{2-}$ (C_{2v} $^1A_1$)	B(2) – Al(4)	0.732	3.477
	B(2) – Be(5)	0.665	
	B(2) – Al(6)	0.682	
$LiBAl_3Be_2^-$ (C_{2v} $^1A_1$)	B(2) – Be(1)	0.649	3.536
	B(2) – Al(3)	0.795	
	B(2) – Al(4)	0.795	
	B(2) – Be(5)	0.649	
	B(2) – Al(6)	0.565	
BAl_3Be_3 (C_{2v} $^1A_1$)	B(2) – Be(1)	0.639	3.598
	B(2) – Al(3)	0.815	
	B(2) – Al(4)	0.815	
	B(2) – Be(5)	0.639	
	B(2) – Al(6)	0.404	
$BAl_2Be_3^{3-}$ (C_{2v} $^1A_1$)	B(2) – Be(1)	0.655	3.523
	B(2) – Al(3)	0.772	
	B(2) – Be(4)	0.669	
	B(2) – Al(5)	0.772	
	B(2) – Be(6)	0.655	
$BAl_2Be_4^-$ (C_s $^1A'$)	B(2) – Be(1)	0.628	3.623
	B(2) – Al(3)	0.752	
	B(2) – Be(4)	0.657	
	B(2) – Al(5)	0.535	
	B(2) – Be(6)	0.806	
$BAl_2Be_5^+$ (C_s $^1A'$)	B(2) – Be(1)	0.803	3.625
	B(2) – Al(3)	0.442	
	B(2) – Be(4)	0.762	
	B(2) – Al(5)	0.645	
	B(2) – Be(6)	0.760	
$BAlBe_4^{4-}$ (C_{2v} $^1A_1$)	B(2) – Be(1)	0.731	3.692
	B(2) – Al(3)	0.800	
	B(2) – Be(4)	0.715	
	B(2) – Be(5)	0.715	
	B(2) – Be(6)	0.731	
$BAlBe_6$ (C_s $^1A'$)	B(7) – Be(1)	0.622	3.691
	B(7) – Be(3)	0.769	
	B(7) – Be(4)	0.705	
	B(7) – Be(5)	0.657	

	B(7) – Al(8)	0.677	
BBe_5^{5-} (D_{5h} $^1A_1'$)	B(2) – Be(1)	0.812	4.062
	B(2) – Be(3)	0.812	
	B(2) – Be(4)	0.812	
	B(2) – Be (5)	0.812	
	B(2) – Be(6)	0.812	
BBe_7^- (C_{2v} $^1A_1$)	B(8) – Be(1)	0.699	3.689
	B(8) – Be(2)	0.592	
	B(8) – Be(4)	0.699	
	B(8) – Be (5)	0.704	
	B(8) – Be(6)	0.704	

Table S14: The studied clusters, their point groups (PG), total energies (E, au), number of imaginary frequency (NIMAG), minimum frequency (ν_{min}, cm^{-1}), HOMO-LUMO gap (Gap, eV) and vertical electron detachment energy for HOMO electron (VEDE*, eV) at B3LYP/6-311+G(d) level

Clusters	PG	E	NIMAG	ν_{min}	Gap	VEDE
BAl_5 ($^1A_1'$)	D_{5h}	-1237.04269	0	73.2	1.900	
BAl_4Be^- ($^1A_1$)	C_{2V}	-1009.40822	0	72.1	1.941	2.801
$LiBAl_4Be$ ($^1A'$)	C_s	-1016.88265	0	22.4	1.939	
$LiBAl_4Be$ ($^1A_1$)	C_{2V}	-1016.87579	0	41.8	1.578	
$BAl_4Be_2^+$ ($^1A'$) [1]	C_s	-1023.82723	0	19.4	2.524	
$BAl_4Be_2^+$ ($^1A'$) [2]	C_s	-1023.82679	0	24.9	2.315	
$BAl_4Be_2^+$ ($^1A_1$)	C_{2V}	-1023.80285	0	64.8	1.513	
$BAl_3Be_2^{2-}$ ($^1A_1$) [1]	C_{2v}	-781.62043	0	101.3	2.033	-0.984
$BAl_3Be_2^{2-}$ ($^1A_1$) [2]	C_{2v}	-781.61110	0	99.2	1.645	
$LiBAl_3Be_2^-$ ($^1A_1$)	C_{2v}	-789.22898	0	53.7	1.879	2.501
$LiBAl_3Be_2^-$ ($^1A'$) [1]	C_s	-789.22208	0	29.1	1.623	
$LiBAl_3Be_2^-$ ($^1A'$) [2]	C_s	-789.22822	0	39.7	1.781	
BAl_3Be_3 ($^1A_1$)	C_{2v}	-796.32833	0	41.2	2.214	
BAl_3Be_3 ($^1A'$)	C_s	-796.31789	0	45.9	1.582	
$BAl_2Be_3^{3-}$ ($^1A_1$) [1]	C_{2v}	-553.70377	0	134.7	1.100	-4.120
$BAl_2Be_3^{3-}$ ($^1A_1$) [2]	C_{2v}	-553.70077	0	179.4	1.139	
$BAl_2Be_4^-$ ($^1A'$) [1]	C_s	-568.68404	0	60.1	2.173	2.879
$BAl_2Be_4^-$ ($^1A'$) [2]	C_s	-568.66735	0	73.9	1.578	
$BAl_2Be_4^-$ ($^1A_1$)	C_{2v}	-568.68163	0	34.6	1.729	
$BAl_2Be_5^+$ ($^1A'$) [1]	C_s	-583.10428	0	42.1	1.761	
$BAl_2Be_5^+$ ($^1A'$) [2]	C_s	-583.10139	0	22.8	1.637	
$BAl_2Be_5^+$ ($^1A'$) [3]	C_s	-583.08735	1	64.7i	1.639	
$BAl_2Be_5^+$ ($^1A'$) [4]	C_s	-583.08568	1	96.0i	2.083	

$BAl_2Be_5^+$ ($^1A'$) [5]	C_s	-583.07957	1	47.4i	1.537	
$BAlBe_4^{4-}$ ($^1A_1$)	C_{2v}	-325.70667	0	219.5	0.725	-6.755
$BAlBe_6$ ($^1A'$) [1]	C_s	-355.59883	0	57.2	1.547	
$BAlBe_6$ ($^1A'$) [2]	C_s	-355.59336	1	76.6i	1.534	
$BAlBe_6$ ($^1A_1$)	C_{2v}	-355.56082	1	46.2i	1.524	
BBe_5^{5-} ($^1A_1'$)	D_{5h}	-97.62522	0	215.2	0.683	-8.918
BBe_7^- ($^1A_1$) [1]	C_{2v}	-127.94990	0	76.9	1.606	2.678
BBe_7^- ($^1A_1$) [1]	C_{2v}	-127.93197	1	38.9i	1.582	

*VEDE is calculated at OVGF/6-311+G(d) level.

Table S15: The nucleus independent chemical shift (NICS (n), ppm) calculated in a triangular plane of the studied clusters at B3LYP/6-311+G(d) level

Clusters	Planes	NICS(0)	NICS(1)	NICS(2)
BAl_5 ($^1A_1'$ D_{5h})	Al(2)-Al(6)-B(1)	-23.578	-23.884	-12.070
BAl_4Be^- (C_{2V} $^1A_1$)	Al(3)-Al(6)-B(2)	-16.216	-18.059	-9.497
	Al(6)-B(2)-Be(1)	-15.642	-19.511	-9.728
$LiBAl_4Be$ (C_s $^1A'$)	Al(3)-Al(6)-B(2)	-21.489	-22.047	-10.951
	Al(6)-B(2)-Be(1)	-20.684	-21.982	-10.857
$BAl_4Be_2^+$ (C_s $^1A'$)	Al(4)-Al(5)-B(2)	-24.393	-19.520	-7.466
	Al(4)-Al(5)-Be(7)	-5.751	-7.542	-4.115
$BAl_3Be_2^{2-}$ (C_{2v} $^1A_1$)	Al(3)-Al(4)-B(2)	-16.908	-18.510	-9.770
	Al(6)-Be(1)-B(2)	-14.450	-16.841	-9.029
$LiBAl_3Be_2^-$ (C_{2v} $^1A_1$)	Al(3)-Al(4)-B(2)	-20.097	-18.402	-8.335
	Al(6)-Be(1)-B(2)	-11.493	-13.079	-6.733
BAl_3Be_3 (C_{2v} $^1A_1$)	Al(3)-Al(4)-B(2)	-25.809	-20.479	-8.059
	Al(3)-Al(4)-Be(7)	-10.166	-11.264	-5.692
$BAl_2Be_3^{3-}$ (C_{2v} $^1A_1$)	Al(3)-Be(4)-B(2)	-13.872	-17.349	-9.132
	B(2)-Be(1)-Be(6)	-12.363	-18.452	-9.498
$BAl_2Be_4^-$ (C_s $^1A'$)	Al(3)-Be(6)-B(2)	-21.248	-19.264	-8.080
	Al(3)-Be(6)-Be(7)	-4.998	-9.014	-5.376
$BAl_2Be_5^+$ (C_s $^1A'$)	Al(5)-Be(4)-B(2)	-16.049	-15.577	-6.769
	Al(5)-Be(4)-Be(8)	-1.613	-5.132	-3.346
$BAlBe_4^{4-}$ (C_{2v} $^1A_1$)	Al(3)-Be(4)-B(2)	-15.716	-15.820	-7.378
	Be(1)-Be(6)-B(2)	-17.771	-12.918	-5.068

$BAlBe_6$ (C_s $^1A'$)	Al(8)-Be(3)-B(7)	-21.660	-8.492	-7.711
	Al(8)-Be(3)-B(6)	-5.106	-8.030	-4.651
BBe_5^{5-} (D_{5h} $^1A_1'$)	B(2)-Be(3)-Be(6)	-20.887	-19.834	-9.393
BBe_7^- (C_{2v} $^1A_1$)	B(8)-Be(4)-Be(6)	-18.284	-17.211	-7.166
	Be(7)-Be(4)-Be(6)	1.853	-4.460	-3.503

Table S16: Total energy (E) of M^{n+}@ (-H_2O, -NH_3, -HF): (M = Li, Na, Be, Mg: n = 1,2) at different level of theory.

Structure	**B3LYP**	**MP2**	**M052X**
	6-311+G(d, p)	**6-311+G(d, p)**	**6-311+G(d, p)**
Li^+-H_2O	-83.8017584	-83.5671307	-83.785722
Na^+-H_2O	-238.587154	-237.978355	-238.561303
Be^{2+}-H_2O	-90.3466556	-90.1109151	-90.337075
Mg^{2+}-H_2O	-275.831201	-275.222666	-275.807812
Li^+-NH_3	-63.9337791	-63.7159369	-63.9157541
Na^+-NH_3	-218.716995	-218.124255	-218.688868
Be^{2+}-NH_3	-70.5101413	-70.2920997	-70.4974508
Mg^{2+}-NH_3	-255.983516	-255.38936	-255.9563
Li^+-HF	-107.80581	-107.55136	-107.792943
Na^+-HF	-262.597787	-261.967555	-262.575075
Be^{2+}-HF	-114.295914	-114.04059	-114.289941
Mg^{2+}-HF	-299.812421	-299.185178	-299.792714

Table S17: Single point energy (E) of M^{n+}@ (-H_2O, -NH_3, -HF): (M = Li, Na, Be, Mg: n 1,2) at different level of theory.

Structure	M052X		MP2(FULL)		CCSD(T)	
	6-311++g(2d,2p)	6-311++g(3d,3p)	6-311++g(2d,2p)	6-311++g(3d,3p)	6-31+g(d)	6-311++g(d,p)
Li^+-H_2O	-83.78708	-83.78791	-83.62028	-83.62556	-83.51361	-83.57858
Na^+-H_2O	-238.56264	-238.56359	-238.15256	-238.17366	-237.92086	-237.98970
Be^{2+}-H_2O	-90.34138	-90.34210	-90.16796	-90.17317	-90.06060	-90.12244
Mg^{2+}-H_2O	-275.81092	-275.81288	-275.39228	-275.40751	-275.16158	-275.23373
Li^+-NH_3	-63.91800	-63.91854	-63.76577	-63.76979	-63.68380	-63.73500
Na^+-NH_3	-218.69107	-218.69190	-218.29534	-218.31529	-218.08781	-218.14314
Be^{2+}-NH_3	-70.50079	-70.50114	-70.34343	-70.34711	-70.26352	-70.31138
Mg^{2+}-NH_3	-255.95978	-255.96097	-255.55559	-255.56920	-255.34934	-255.40804
Li^+-HF	-107.79410	-107.79479	-107.60920	-107.61525	-107.47976	-107.55750
Na^+-HF	-262.57630	-262.57694	-262.14802	-262.16964	-261.89149	-261.97271
Be^{2+}-HF	-114.29570	-114.29699	-114.10404	-114.11052	-113.97439	-114.04657
Mg^{2+}-HF	-299.79541	-299.79701	-299.35950	-299.37505	-299.10577	-299.19119

Table S18: Electronegativity (χ, eV), hardness (η, eV) and electrophilicity (ω, eV) values and NPA charge on metal center (Q_M) of M^{n+}@ (-H_2O, -NH_3, -HF): (M = Li, Na, Be, Mg: n = 1,2) at B3LYP /6-311+G(d, p) level of theory

Structure	χ	η	ω	Q_M
Li^+-H_2O	12.196	15.067	4.936	0.99061
Na^+-H_2O	11.636	14.063	4.814	0.99751
Be^{2+}-H_2O	22.301	14.802	16.801	1.8961
Mg^{2+}-H_2O	19.758	13.036	14.973	1.97358
Li^+-NH_3	11.560	14.100	4.739	0.97986
Na^+-NH_3	10.910	12.893	4.616	0.98911
Be^{2+}-NH_3	22.238	15.555	15.896	1.84886
Mg^{2+}-NH_3	19.368	13.139	14.276	1.92406
Li^+-HF	14.225	18.775	5.389	0.99501
Na^+-HF	13.614	17.689	5.239	0.99888
Be^{2+}-HF	24.842	18.436	16.738	1.9336
Mg^{2+}-HF	22.053	16.573	14.673	1.98974

Table S19: : Electronegativity (χ, eV), hardness (η, eV) and electrophilicity (ω, eV) values and NPA charge on metal center (Q_M) of M^{n+}@ (-H_2O, -NH_3, -HF): (M = Li, Na, Be, Mg: n = 1,2) at M052X/6-311+G(d, p) level of theory

Structure	χ	η	ω	Q_M
Li^+-H_2O	11.906	15.359	4.614	0.95487
Na^+-H_2O	11.418	14.592	4.467	0.99598
Be^{2+}-H_2O	22.094	15.213	16.043	1.87721
Mg^{2+}-H_2O	19.540	13.586	14.052	1.96372
Li^+-NH_3	10.643	12.348	4.586	0.97482
Na^+-NH_3	10.707	13.362	4.290	0.98298
Be^{2+}-NH_3	22.032	15.950	15.216	1.83840
Mg^{2+}-NH_3	19.161	13.583	13.515	1.90147
Li^+-HF	14.004	19.194	5.109	0.99305
Na^+-HF	13.397	18.258	4.915	0.99842
Be^{2+}-HF	24.615	18.851	16.071	1.91551
Mg^{2+}-HF	21.789	17.104	13.879	1.98516

Table S20: Electronegativity (χ, eV), hardness (η, eV) and electrophilicity (ω, eV) values and NPA charge on metal center (Q_M) of M^{n+}@ (-H_2O, -NH_3, -HF): (M = Li, Na, Be, Mg: n = 1,2) at MP2/6-311+G(d, p) level of theory

Structure	χ	η	ω	Q_M
Li^+-H_2O	11.880	15.117	4.668	0.99061
Na^+-H_2O	11.830	15.604	4.485	0.99751
Be^{2+}-H_2O	21.954	14.772	16.314	1.8961
Mg^{2+}-H_2O	19.284	13.271	14.011	1.97358
Li^+-NH_3	11.269	14.112	4.500	0.97986
Na^+-NH_3	10.553	13.016	4.278	0.98911
Be^{2+}-NH_3	21.931	15.585	15.430	1.84886
Mg^{2+}-NH_3	18.916	13.286	13.467	1.92406
Li^+-HF	13.874	18.788	5.122	0.99501
Na^+-HF	13.154	17.661	4.898	0.99888
Be^{2+}-HF	24.457	18.391	16.262	1.9336
Mg^{2+}-HF	21.458	16.646	13.830	1.98974

Table S21: The total energy (E, au), electronegativity (χ, eV), hardness(η, eV) and electrophilicity (ω, eV) for the possible isomers of Be_8^{2-} molecule at B3LYP/6-311+G(d) level

MOLECULE	E	χ	η	ω
1	-117.76101	-2.844	3.641	1.111
2	-117.77265	-3.103	3.392	1.419
3	-117.74109	-3.102	3.164	1.521
4	-117.80698	-3.177	3.996	1.263
5	-117.76308	-2.963	3.601	1.219
6	-117.78660	-3.125	3.776	1.293
7	-117.80336	-2.994	4.071	1.101
8	-117.79542	-3.297	3.784	1.436
9	-117.66351	-3.209	3.264	1.578
10	-117.73188	-2.921	3.463	1.231
11	-117.74914	-3.227	3.844	1.354
12	-117.75912	-2.694	3.907	0.929
13	-117.76113	-2.958	3.695	1.184
14	-117.58256	-2.342	1.197	2.292
15	-117.78651	-3.390	3.367	1.706

Table S22: Atomic charges (Q_k, au), various bond distances (Å) and bond angles(°) of all the possible isomers of Be_8^{2-} molecule optimized at B3LYP/6-311+G(d) level.

Atomic Charges (NPA)	Bond distances	Bond angles
0.194, -1.363 -0.084, 0.139 -0.136, -0.498 -0.294, 0.043	R(1,2)=R(1,3)=1.997 R(1,4)=R(1,8)=2.100 R(1,5)=1.974; R(2,3)= 2.090 R(3,4)=R(2,8)= 2.450 R(4,5)=R(5,8)=2.093 R(4,6)=R(7,8)=2.024 R(3,6)=R(2,7)= 2.077	A(2,1,3)= 63.083 A(3,1,4)= 73.394 A(2,1,8)= 73.373 A(4,1,5)= 61.751 A(5,1,8)= 61.747 A(3,6,4)= 73.348 A(2,7,8)= 73.332
-0.121, -0.078 0.002, -0.156	R(1,7)= 1.853 R(1,2)=R(2,7)=2.101	A(1,3,7)= 47.988 A(1,2,7)= 52.354

-1.265, -0.002 -0.108, -0.273	R(1,5)= R(5,7)= 2.100 R(2,6)= 2.248; R(4,5)= 2.247 R(6,8)= 2.076; R(4,6)= 2.076 R(2,3)= R(3,5)=1.961 R(3,6)= R(3,4)= 2.043 R(1,3)= R(3,7)= 2.279	A(1,5,7)=52.367 A(2,3,6)=68.287 A(5,3,4)=68.237 A(6,3,8)=56.256 A(4,3,8)= 56.253
-0.403, -0.096 -0.403, -0.403 -0.403, -0.096 -0.097, -0.097	R(1,2)=R(2,3)= 2.189 R(3,8)=R(1,6)= 2.139 R(6,8)= 2.039; R(2,5)= 2.205 R(2,7)= 1.986; R(4,7)= 2.185 R(1,7)= R(3,7)= 1.992 R(4,6)=R(4,8)= 2.015	A(1,2,3)= 69.513 A(1,7,3)= 77.574 A(1,4,3)= 71.100 A(6,4,8)= 60.794 A(1,4,6) = 61.741 A(3,4,8)= 61.779
-0.383, -0.384 -0.117, -0.116 -0.384, -0.383 -0.116, -0.117	R(1,2)= R(1,6)= 2.106 R(2,7)= 2.107; R(6,7)= 2.790 R(2,3)= 2.039; R(1,3)= 2.047 R(3,7)= 2.207; R(3,6)= 2.196 R(7,8)= 2.206; R(6,8)= 2.207 R(1,8)= 2.040; R(2,8)= 2.041 R(4,6)= 2.039; R(4,7)= 2.039 R(5,7)= 2.048; R(5,6)= 2.042	A(1,3,2)= 59.126 A(1,3,6)=59.381 A(6,3,7)= 78.611 A(2,3,7)= 59.343 A(1,8,2)= 59.205 A(1,8,6)= 59.286 A(2,8,7)= 59.346 A(6,8,7)= 78.416 A(6,4,7)= 86.313 A(6,5,7)= 86.011
-0.123, -0.175 -1.298, -0.221 -0.025, 0.186 -0.159, -0.184	R(1,2)=R(1,7)= 2.000 R(1,5)= 1.982; R(2,7)= 2.116 R(5,7)= 2.013; R(2,5)= 2.013 R(2,3)= 2.224; R(3,7)= 2.224 R(3,5)= 2.231; R(3,6)= 2.082 R(3,8)= 2.034; R(3,4)= 2.066 R(2,4)= 2.142; R(4,7)= 2.142	A(2,5,7)= 63.399; A(5,7,2)= 58.299 A(7,2,5)= 58.301; A(2,1,5)= 60.738 A(2,1,7)= 63.867; A(5,1,7)= 60.734 A(3,2,5)= 53.728; A(2,3,7)= 56.806 A(5,3,7)= 53.729; A(2,4,7)= 59.192 A(3,4,8)= 60.211; A(3,6,8)= 59.403 A(3,8,6)= 61.758; A(3,8,4)= 61.851
-0.301, -0.301 -0.227, -0.042 -0.326, -0.325 -0.042, -0.435	R(4,8)= R(7,8) =2.141 R(2,4)= R(1,7)= 1.962 R(4,6)= R(5,7)= 2.015 R(2,6)= R(1,5)=1.953 R(3,6)= R(3,5)= 2.111 R(5,6)= 2.456 R(1,3)=R(2,3)= 2.120	A(2,8,6)= 50.745 A(1,8,5)= 50.706 A(2,3,6)= 54.978 A(1,3,5)= 54.991 A(2,4,6)= 58.802 A(1,7,5)= 58.798 A(5,8,6)= 68.413
-0.104, -0.304 -0.215, -0.105 -0.302, -0.216 -0.375, -0.378	R(1,2)= 1.945; R(1,3)=1.987 R(1,7)= 2.072; R(2,3)= 2.005 R(3,7)= 2.083; R(2,7)= 2.058 R(4,5)= 2.060; R(4,6)= 2.073 R(4,8)= 2.084; R(5,6)= 1.945 R(5,8)= 2.004; R(6,8)= 1.987 R(3,4)= 2.241; (R4,7)= 2.134 R(3,8)= 2.247; R(7,8)= 2.241	A(2,1,3)= 61.317; A(2,1,7)= 61.550 A(3,1,7)= 61.728; A(3,2,7)= 61.674 A(1,4,3)= 52.197; A(1,7,4)= 65.445 A(3,8,7)= 55.322; A(5,6,8)= 61.277 A(6,4,5)= 56.165; A(6,4,8)= 57.094 A(5,4,8)= 57.839; A(4,7,8)=56.843 A(4,7,6)= 55.978; A(6,7,8)= 52.200
-0.265, -0.197 -0.265, -0.268 -0.270, -0.270	R(2,4)=R(3,7) = 2.010 R(2,6)=R(1,7) = 2.011 R(4,6)=R(1,3) = 2.010	A(2,5,4)= A(3,8,7)= 59.832 A(2,5,6)= A(1,8,7)= 59.844 A(4,5,6)= A(1,8,3)= 59.802

-0.197, -0.268	R(1,8)= R(3,8) = 2.016 R(7,8)=R(2,5) = 2.015 R(4,5)=R(4,6) = 2.016	A(2,4,6) = A(1,3,7)=60.017 A(4,2,6)= A(3,7,1)=59.984 A(2,6,4) = A(3,1,7)= 60.000
-0.232, -0.268 -0.232, -0.268 -0.232, -0.268 -0.232, -0.268	R(1,2)= R(2,3)= 2.112 R(3,4)= R(4,5)= 2.112 R(5,6)= R(6,7)= 2.112 R(7,8)= R(8,1)= 2.112	A(1,2,3)= A(5,6,7) =134.953 A(2,3,4)= A(6,7,8)=134.902 A(4,5,6) =A(8,1,2)=134.943 A(3,4,5)= 134.953 A(7,8,1)= 134.953
-0.250, -0.250 -0.246, -0.480 -0.246, -0.480 -0.024, -0.024	R(2,3)= R(1,5)=2.092 R(4,7)=R(6,8)= 2.102 R(2,7)=R(1,8)= 2.010 R(3,5)= 2.034 R(4,6)= 2.210	A(2,3,4)= 74.029; A(1,4,5)= 74.025 A(2,7,4) = 73.134; A(1,8,6)= 73.134 A(3,4,5)= 59.663; A(4,5,6)= 65.444 A(4,3,5)= 63.395; A(4,5,3)= 56.942 A(4,6,5)= 60.156; A(5,6,4)= 60.156
-0.224, -0.064 -0.091, -0.091 0.061, -1.795 0.256, -0.051	R(1,3)=R(1,4)= 1.988 R(2,4)= R(2,3)= 2.044 R(3,4)= 2.143; R(5,6)= 2.243 R(5,7)= 2.123; R(6,8)= 2.068 R(7,8)= 2.054; R(6,7)= 2.101 R(2,6)= 1.947; R(1,5)= 1.983 R(3,6)= R(4,6)=2.208 R(3,5)=R(4,5)= 2.169	A(3,2,4)=A(3,1,4)= 65.216 A(2,3,4)= A(2,4,3)=58.375 A(1,3,4)= A(1,4,3)=57.392 A(5,6,7)= 58.414; A(7,6,8)= 59.020 A(6,7,8)= 59.710; A(6,7,5)= 64.147 A(6,5,7)= 57.438; A(6,8,7)= 61.271 A(3,6,4)= 58.069; A(3,5,4)= 59.227
-0.193, -0.422 -0.421, -0.193 -0.193, -0.192 -0.192, -0.193	R(1,7)=R(7,8)=R(8,1)= 2.009 R(4,5)=R(5,6)=R(4,6)= 2.009 R(3,4)=R(3,5)=R(3,6)= 2.103 R(2,1)=R(2,7)=R(2,8)= 2.103 R(2,3)= 2.175	A(1,7,8)= 60.000 A(7,8,1)= 60.000 A(7,1,8)=60.000 A(4,5,6)= 60.000 A(5,6,4)= 60.000 A(6,4,5)=60.000
-0.919, -0.252 -0.252, -0.422 0.091, 0.088 0.089, -0.423	R(2,3)= 2.090; R(1,5)= 1.974 R(3,4)= 2.450; R(2,8)= 2.450 R(4,5)=R(5,8)= 2.093 R(1,2)= R(1,3)=1.998 R(1,4)=R(1,8)= 2.100 R(3,6)= R(2,7)=2.077 R(4,6)= R(7,8)= 2.024	A(3,6,4)= 73.348 A(2,7,8)= 73.332 A(2,1,3)= 63.083 A(3,1,4)= 73.394 A(4,1,5)= 61.751 A(5,1,8)= 61.747 A(2,1,8)= 73.373
-0.171, -0.229 -0.131, -0.244 -0.277, -0.319 -0.276, -0.338	R(1,2)=R(1,3)= 2.105 R(2,5)=R(3,6)= 2.075 R(6,7)=R(5,8)= 2.100	A(7,6,4)= A(6,4,3)=180.000 A(4,3,1)= A(3,1,2)=180.000 A(1,2,5)=180.000
-0.108, -0.407 -0.027, -0.460 -0.364, -0.123 -0.226, -0.283	R(1,5)=R(5,8)= 2.006 R(2,4)=R(4,8)= 2.084 R(6,7)=R(2,7)= 2.004 R(1,3)=R(3,6)= 2.084	A(6,7,2)= 72.850 A(2,4,8)= 62.466 A(8,5,1)= 2.763 A(1,3,6)= 62.468 A(4,2,7)= 62.852 A(3,6,7)= 62.853

		A(3,1,5)= 62.861 A(5,8,4)= 62.861

Table S23: Total energy (E, au), Point groups (PG), Ionization energy (IP, eV)), Electron affinity (EA, eV), Electronegativity (χ, eV)),Hardness(η, eV)),Electrophilicity(ω, eV)) of optimized structures at HF/6-311+G(d) level

Clusters	E	PG	IP	EA	χ	η	ω
$[(B_3BO_3)_2N_4Be_2]^{2-}$	-992.97726	C_s	4.057	-4.843	-0.393	8.900	0.009
$[(B_3BO_3)_2N_5Be_2]^{-}$	-1047.47625	C_1	7.886	-1.502	3.192	9.388	0.543
$[(B_3BO_3)_2N_6Be_2]^{2-}$	-1101.89746	C_1	4.449	-4.735	-0.143	9.184	0.001
$[(B_3BO_3)_2P_4Be_2]^{2-}$	-2138.23555	C_s	3.665	-4.233	-0.284	7.898	0.005
$[(B_3BO_3)_2CpBe_2]^{-}$	-967.48493	C_2	6.937	-2.664	2.136	9.602	0.238
$[(B_3BO_3)_2Be_5]^{2-}$	-819.00970	D_{3h}	2.998	-4.103	-0.552	7.102	0.021
$[(B_3BO_3)_2Mg_3Be_2]^{2-}$	-1374.04798	C_{2v}	1.442	-3.786	-1.172	5.228	0.131
	-1373.99178	D_{3h}					
$[(B_3BO_3)_2Mg_3Be_2]^{2-}$		(2)	1.910	-3.768	-0.929	5.678	0.076
$[(B_3BO_3)_2Al_4Be_2]^{2-}$	-1742.89507	C_1	2.453	-3.684	-0.616	6.137	0.031
	-1742.87315	Cs					
$[(B_3BO_3)_2Al_4Be_2]^{2-}$		(1)	2.444	-3.542	-0.549	5.987	0.025

For the structures in which there exists imaginary frequency, is given in bracket below point group.

Table S24: Total energy (E, au), Point groups (PG), Ionization energy (IP, eV)), Electron affinity (EA, eV), Electronegativity (χ, eV)),Hardness(η, eV)),Electrophilicity(ω, eV)) of optimized structures at B3LYP/6-311+G(d) level

Clusters	E	PG	IP	EA	χ	η	ω
$[(B_3BO_3)_2N_4Be_2]^{2-}$	-998.73602	C_s	2.784	-3.555	-0.385	6.339	0.012
$[(B_3BO_3)_2N_5Be_2]^{-}$	-1053.51404	C_1	6.548	0.690	3.619	5.858	1.118
	-1108.26883	C_1					
$[(B_3BO_3)_2N_6Be_2]^{2-}$		(1)	2.992	-3.054	-0.031	6.046	0.000
$[(B_3BO_3)_2P_4Be_2]^{2-}$	-2145.32675	C_s	2.4598	-2.897	-0.219	5.357	0.004
$[(B_3BO_3)_2CpBe_2]^{-}$	-973.28661	C_2	5.675	-0.552	2.562	6.227	0.527
$[(B_3BO_3)_2Be_5]^{2-}$	-823.91669	D_{3h}	2.256	-2.935	-0.339	5.191	0.011
$[(B_3BO_3)_2Mg_3Be_2]^{2}$	-1380.02218						
-		D_{3h}	1.894	-3.011	-0.559	4.905	0.032
$[(B_3BO_3)_2Al_4Be_2]^{2-}$	-1749.59078	C_s	2.050	-2.599	-0.274	4.649	0.008

For the structures in which there exists imaginary frequency, is given in bracket below point group.

Table S25: Total energy (E, au), Point groups (PG), Ionization energy (IP, eV)), Electron affinity (EA, eV), Electronegativity (χ, eV)),Hardness(η, eV)),Electrophilicity(ω, eV)) of optimized structures at M052X/6-311+G(d) level

Clusters	E	PG	IP	EA	χ	η	ω
$[(B_3BO_3)_2N_4Be_2]^{2-}$	-998.62810	C_s	3.388.	.-4.022	-0.317	7.410	0.007
$[(B_3BO_3)_2N_5Be_2]^{-}$	-1053.38780	C_1	7.181	0.476	3.829	6.704	1.093
$[(B_3BO_3)_2N_6Be_2]^{2-}$	-1108.13590	C_1	3.665	-3.339	0.163	7.004	0.002
$[(B_3BO_3)_2P_4Be_2]^{2-}$	-2145.18545	C_s	2.918	-3.433	-0.257	6.350	0.005
$[(B_3BO_3)_2CpBe_2]^{-}$	-973.20572	C_2	6.144	-0.802	2.671	6.946	0.514
$[(B_3BO_3)_2Be_5]^{2-}$	-823.82294	D_{3h}	2.587	-2.975	-0.194	5.562	0.003
$[(B_3BO_3)_2Mg_3Be_2]^{2-}$	-1379.88882	D_{3h}	2.105	-2.973	-0.434	5.078	0.018
$[(B_3BO_3)_2Al_4Be_2]^{2-}$	-1749.49298	C_s	1.925	-3.119	-0.597	5.044	0.035

Table S26: The NICS(0) values in ppm unit of the double decker sandwhich complexes studied at B3LYP/6-311+G(d) level

CLUSTERS	NICS(0)	CLUSTERS	NICS(0)	CLUSTERS	NICS(0)
$[(B_3BO_3)_2N_4Be_2]^{2-}$	-3.430	$[(B_3BO_3)_2P_4Be_2]^{2-}$	-12.949	$[(B_3BO_3)_2Mg_3Be_2]^{2-}$	7.942
	7.081		-3.613		-17.566
	-1.483		-12.949		7.942
$[(B_3BO_3)_2N_5Be_2]^{-}$	16.194	$[(B_3BO_3)_2CpBe_2]^{-}$	-9.351	$[(B_3BO_3)_2Al_4Be_2]^{2-}$	1.343
	-16.669		-21.653		-23.325
	12.427		-10.298		-41.886
$[(B_3BO_3)_2N_6Be_2]^{2-}$	0.747	$[(B_3BO_3)_2Be_5]^{2-}$	-1.096		
	2.060		-24.438		
	0.154		-1.096		

Upper NICS(0) values corresponds to upper ring, middle NICS(0) values corresponds to middle ring and lower NICS(0) values corresponds to lower ring

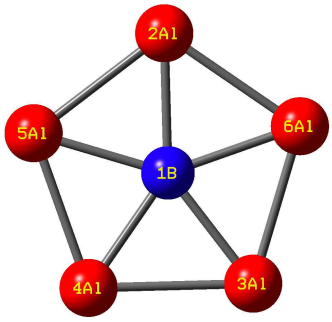

BAl_5 (D_{5h} $^1A_1'$)

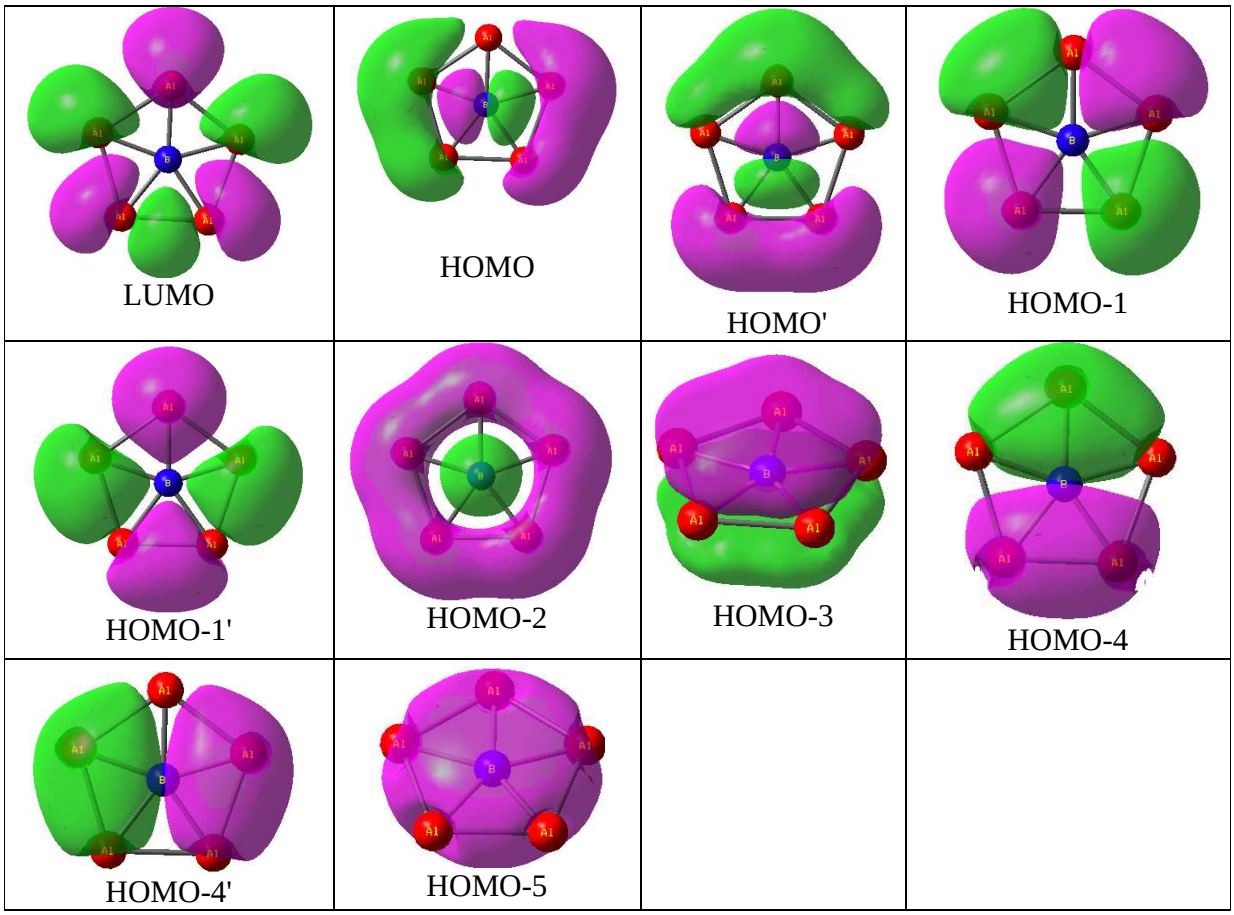

Fig. S1. The optimized geometry of BAl_5 (D_{5h} $^1A_1'$) and its lowest unoccupied molecular orbital as well as all occupied valence molecular orbitals at B3LYP/6-311+G(d) level.

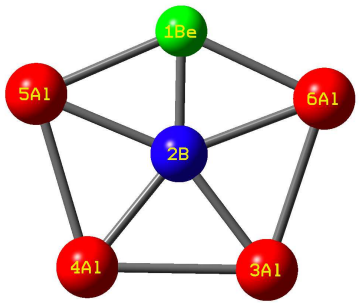

BAl_4Be^- (C_{2V} $^1A_1$)

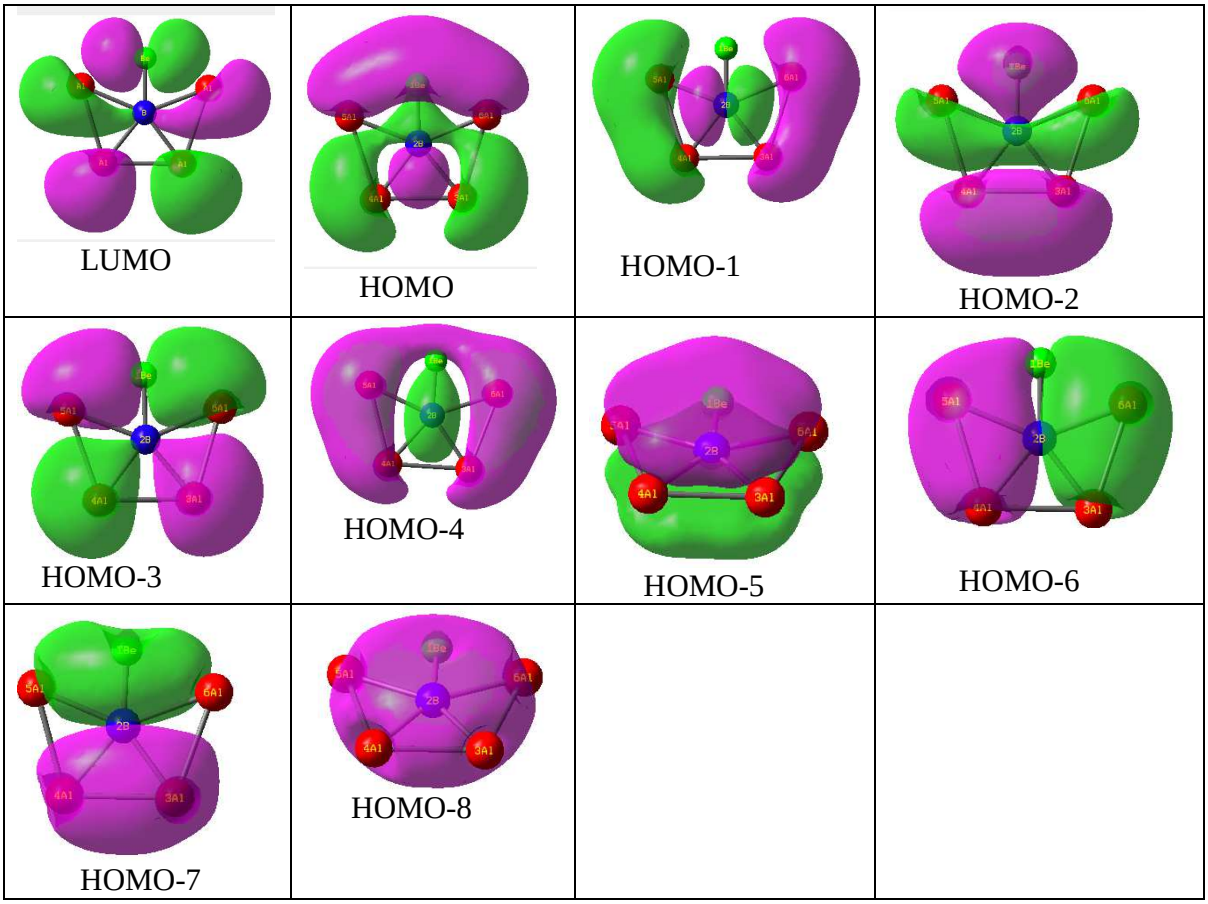

Fig. S2. The optimized geometry of BAl_4Be^- (C_{2V} $^1A_1$) and its lowest unoccupied molecular orbital as well as all occupied valence molecular orbitals at B3LYP/6-311+G(d) level.

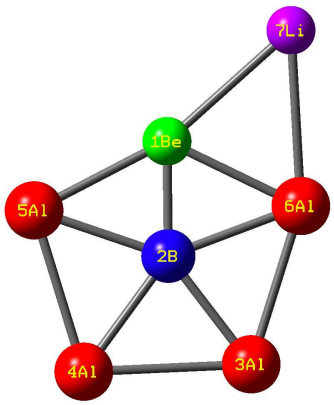

$LiBAl_4Be$ (C_s $^1A'$)

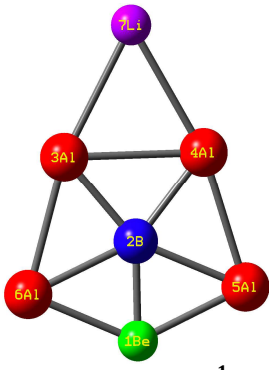

$LiBAl_4Be$ (C_{2V} $^1A_1$)

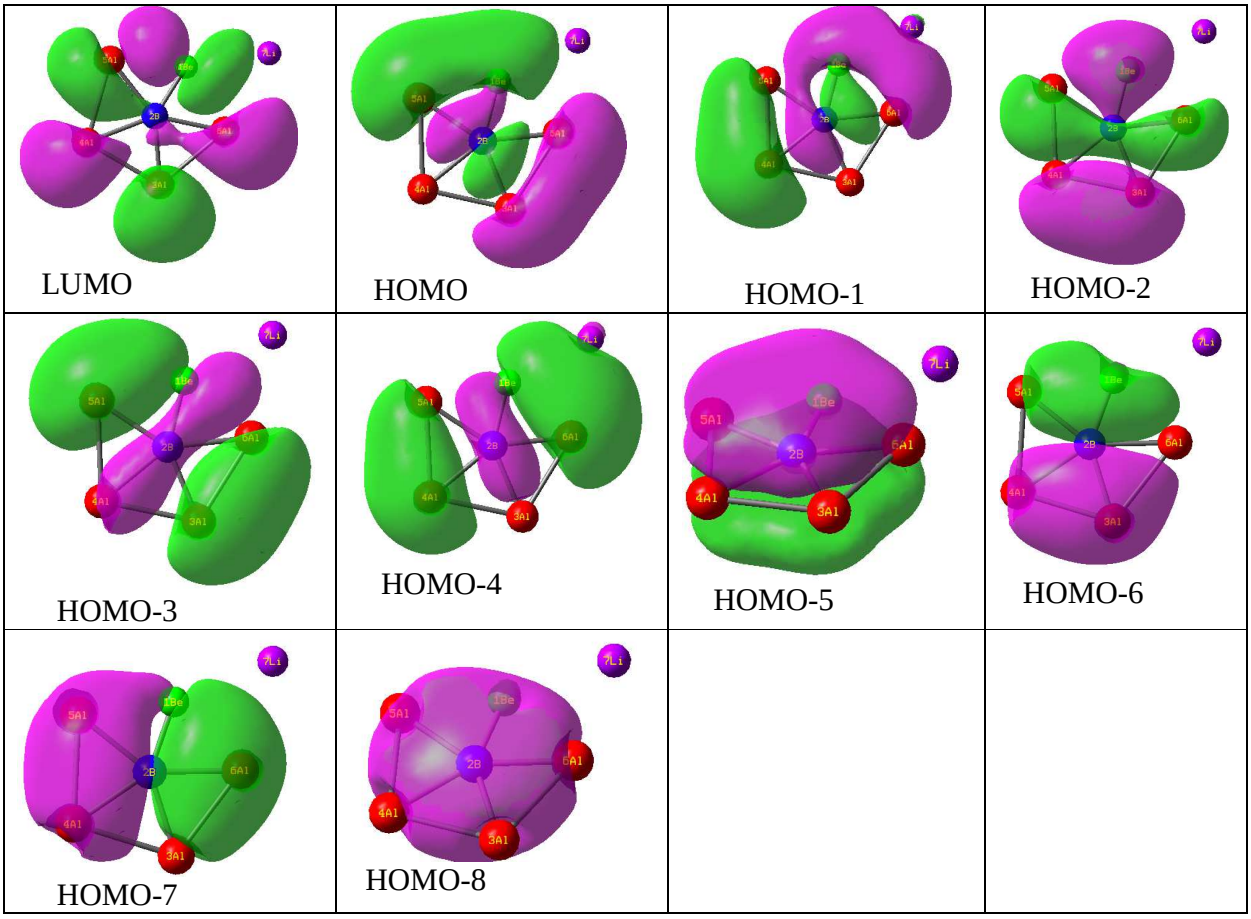

Fig. S3. The optimized geometries of $LiBAl_4Be$ and the lowest unoccupied molecular orbital as well as all occupied valence molecular orbitals of $LiBAl_4Be$ (C_s $^1A'$) at B3LYP/6-311+G(d) level.

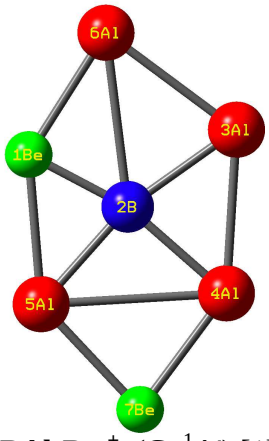

$BAl_4Be_2^+$ (C_s $^1A'$) [1]

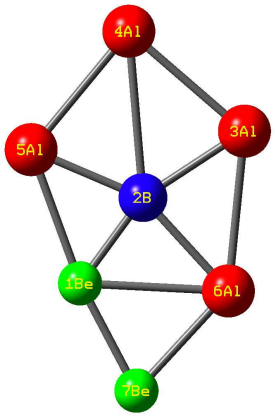

$BAl_4Be_2^+$ (C_s $^1A'$) [2]

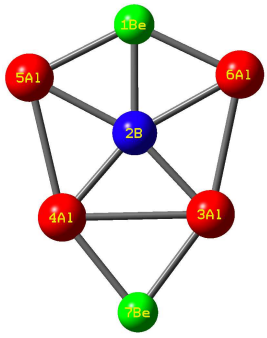

$BAl_4Be_2^+$ (C_{2v} $^1A_1$)

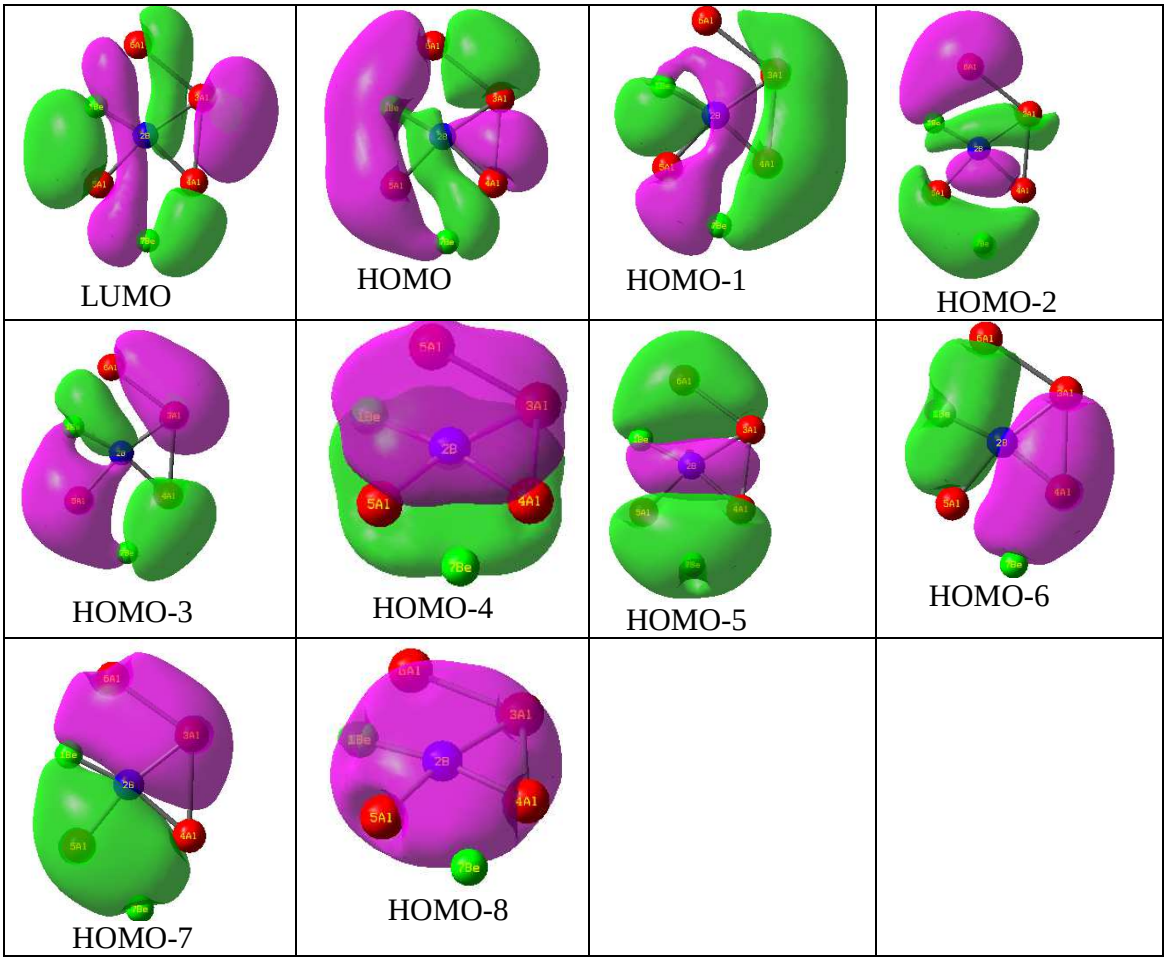

Fig. S4. The optimized geometries of $BAl_4Be_2^+$ and the lowest unoccupied molecular orbital as well as all occupied valence molecular orbitals of $BAl_4Be_2^+$ (C_s $^1A'$) [1] at B3LYP/6-311+G(d) level.

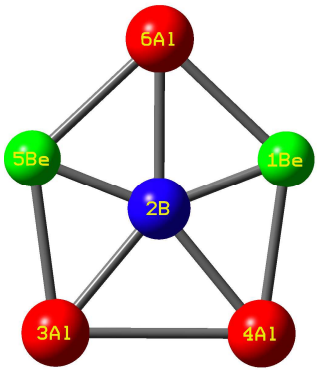

$BAl_3Be_2^{2-}$ (C_{2v} $^1A_1$) [1]

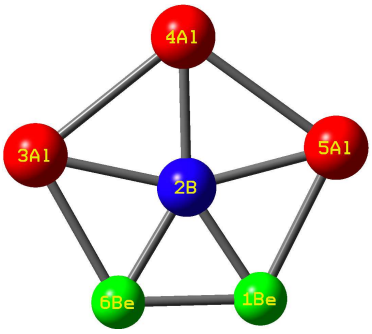

$BAl_3Be_2^{2-}$ (C_{2v} $^1A_1$) [2]

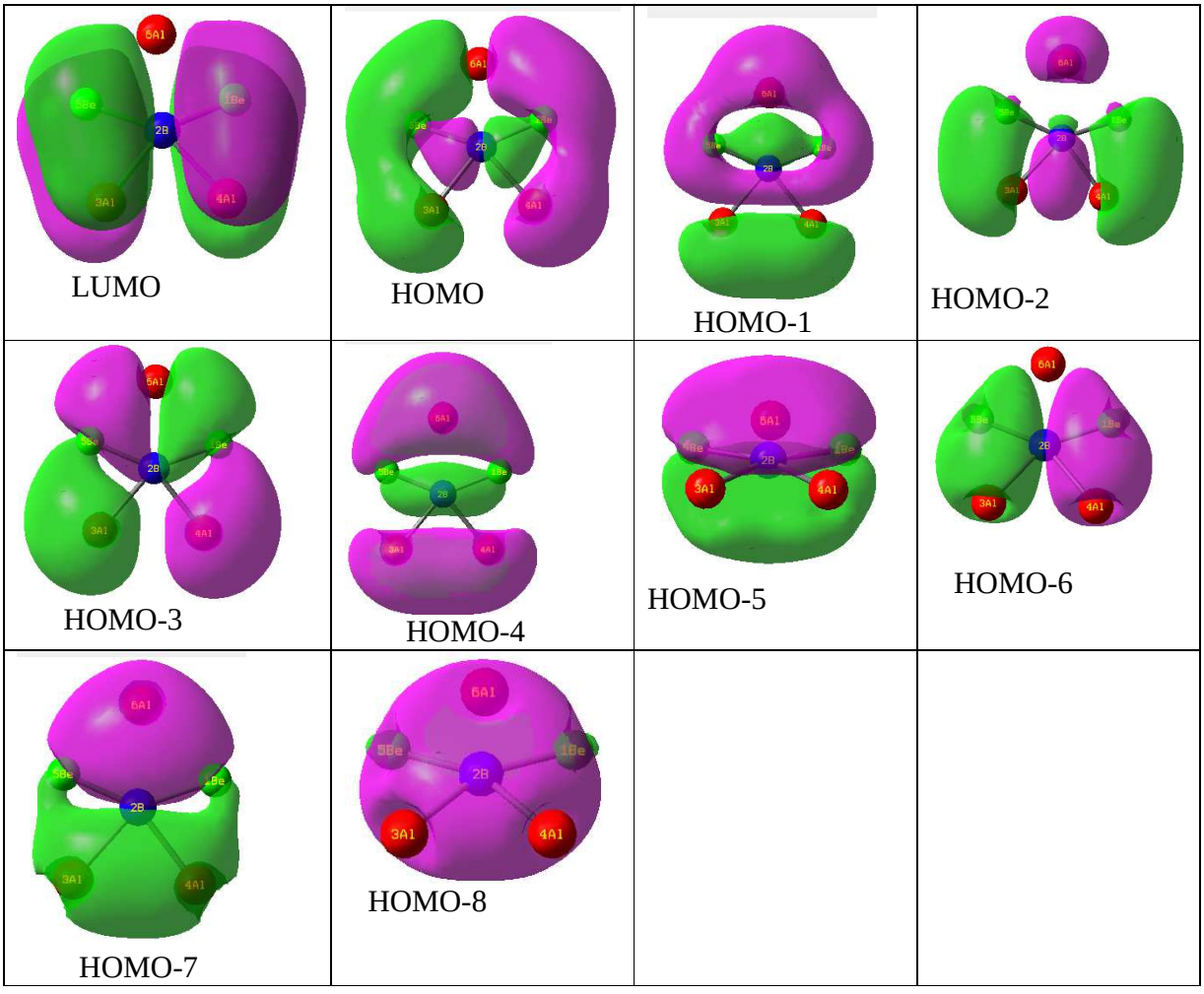

Fig. S5. The optimized geometries of $BAl_3Be_2^{2-}$ and the lowest unoccupied molecular orbital as well as all occupied valence molecular orbitals of $BAl_3Be_2^{2-}$ (C_{2v} $^1A_1$) [1] at B3LYP/6-311+G(d) level.

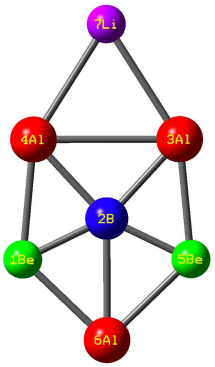

$LiBAl_3Be_2^-$ (C_{2v} $^1A_1$)

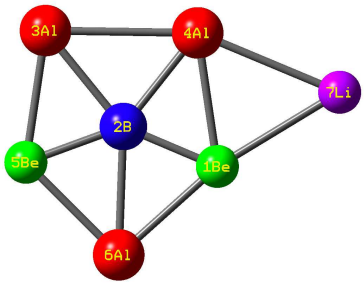

$LiBAl_3Be_2^-$ (C_s $^1A'$) [1]

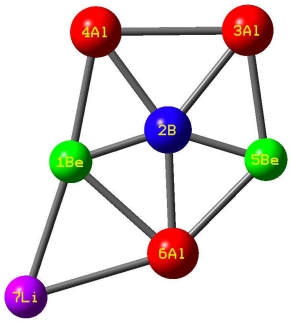

$LiBAl_3Be_2^-$ (C_s $^1A'$) [2]

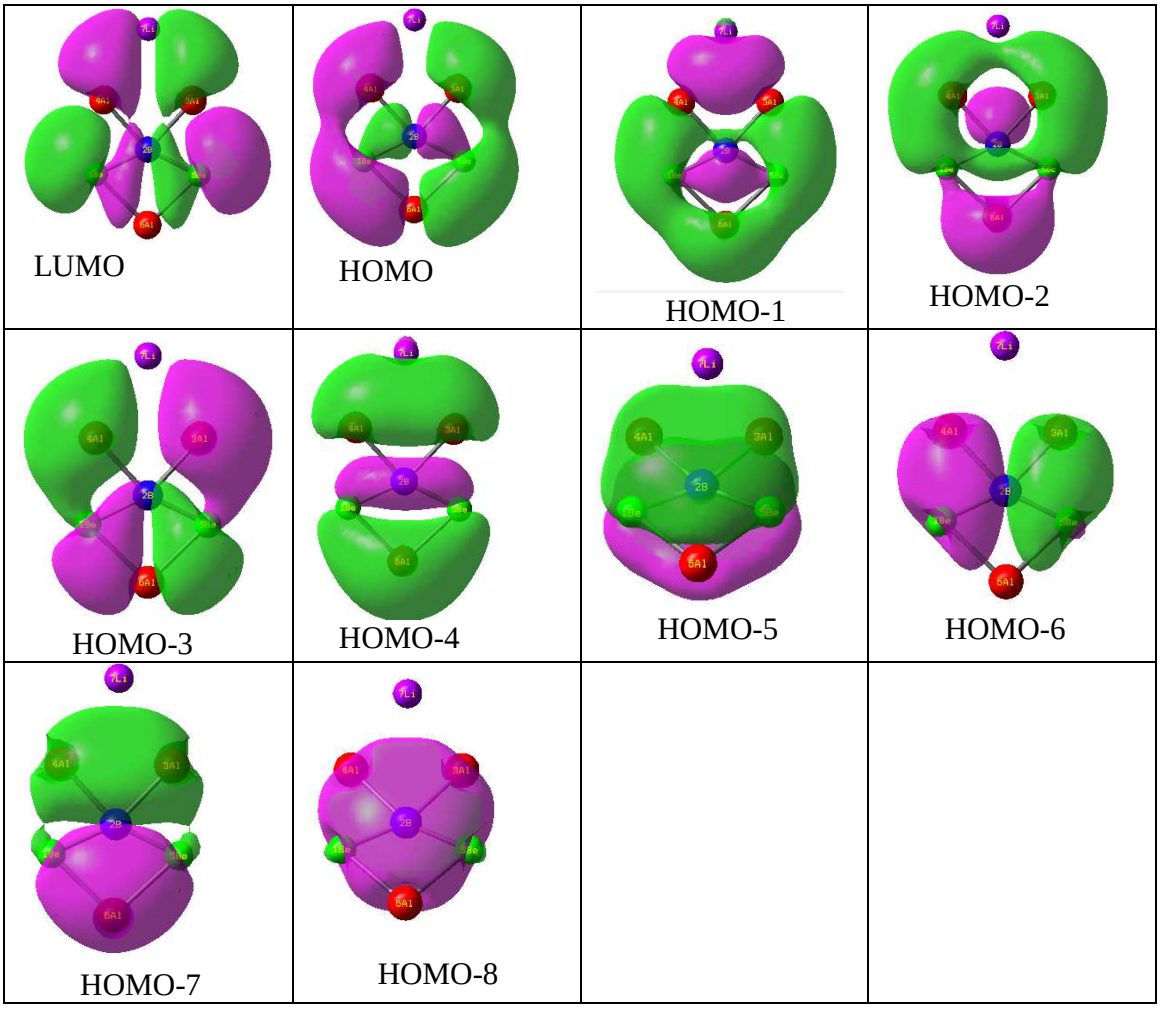

Fig. S6. The optimized geometries of $LiBAl_3Be_2^-$ and the lowest unoccupied molecular orbital as well as all occupied valence molecular orbitals of $LiBAl_3Be_2^-$ (C_{2v} $^1A_1$) at B3LYP/6-311+G(d) level.

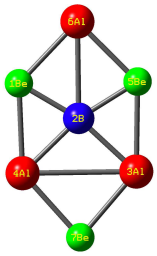

BAl_3Be_3 (C_{2v} $^1A_1$)

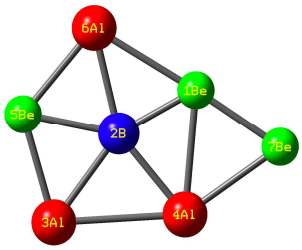

BAl_3Be_3 (C_s $^1A'$)

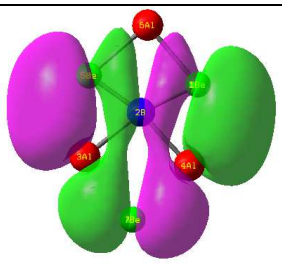

LUMO

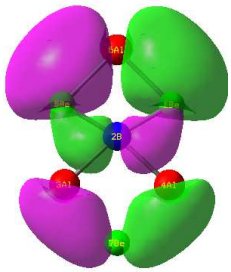

HOMO

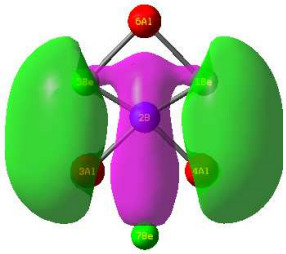

HOMO-1

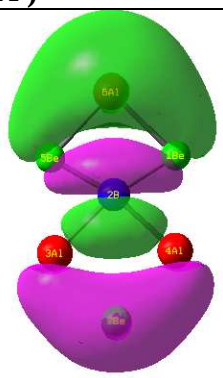

HOMO-2

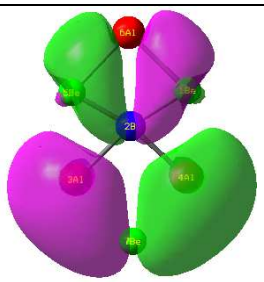

HOMO-3

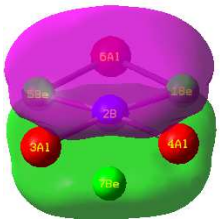

HOMO-4

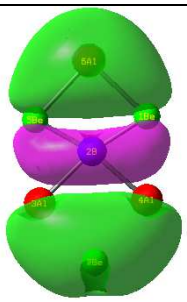

HOMO-5

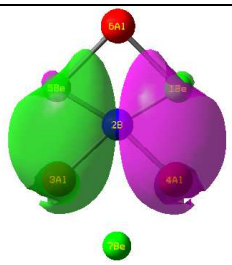

HOMO-6

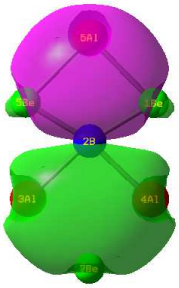

HOMO-7

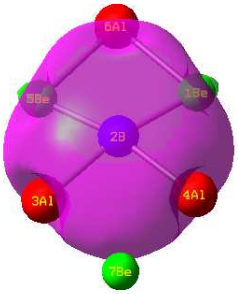

HOMO-8

Fig. S7. The optimized geometries of BAl_3Be_3 and the lowest unoccupied molecular orbital as well as all occupied valence molecular orbitals of BAl_3Be_3 (C_{2v} $^1A_1$) at B3LYP/6-311+G(d) level.

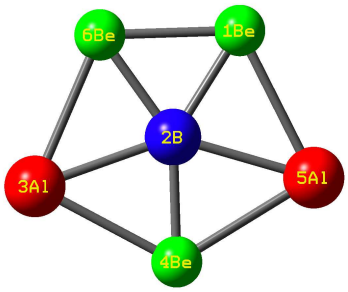

$BAl_2Be_3^{3-}$ (C_{2v} $^1A_1$) [1]

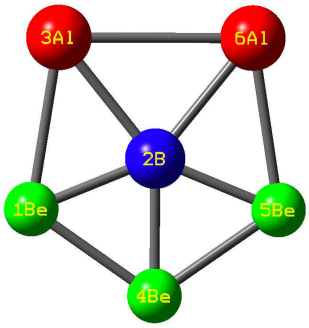

$BAl_2Be_3^{3-}$ (C_{2v} $^1A_1$) [2]

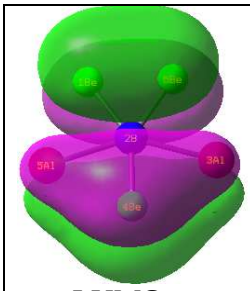

LUMO

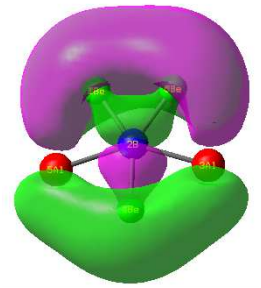

HOMO

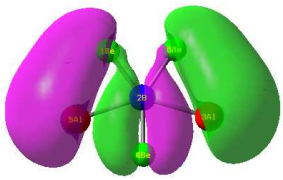

HOMO-1

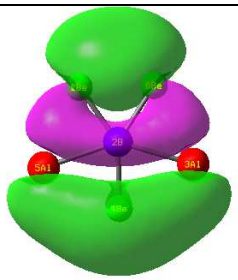

HOMO-2

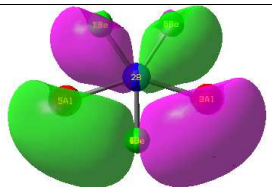

HOMO-3

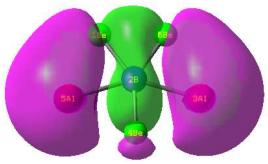

HOMO-4

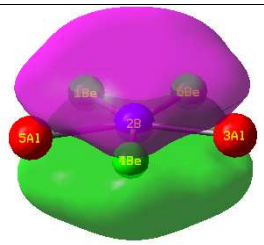

HOMO-5

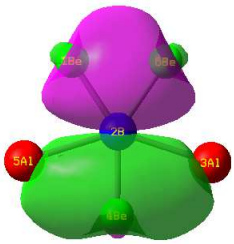

HOMO-6

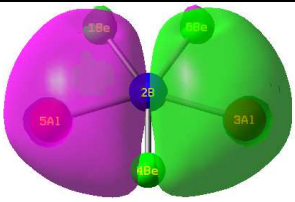

HOMO-7

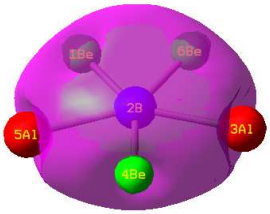

HOMO-8

Fig. S8. The optimized geometries of $BAl_2Be_3^{3-}$ and the lowest unoccupied molecular orbital as well as all occupied valence molecular orbitals of $BAl_2Be_3^{3-}$ (C_{2v} $^1A_1$) [1] at B3LYP/6-311+G(d) level.

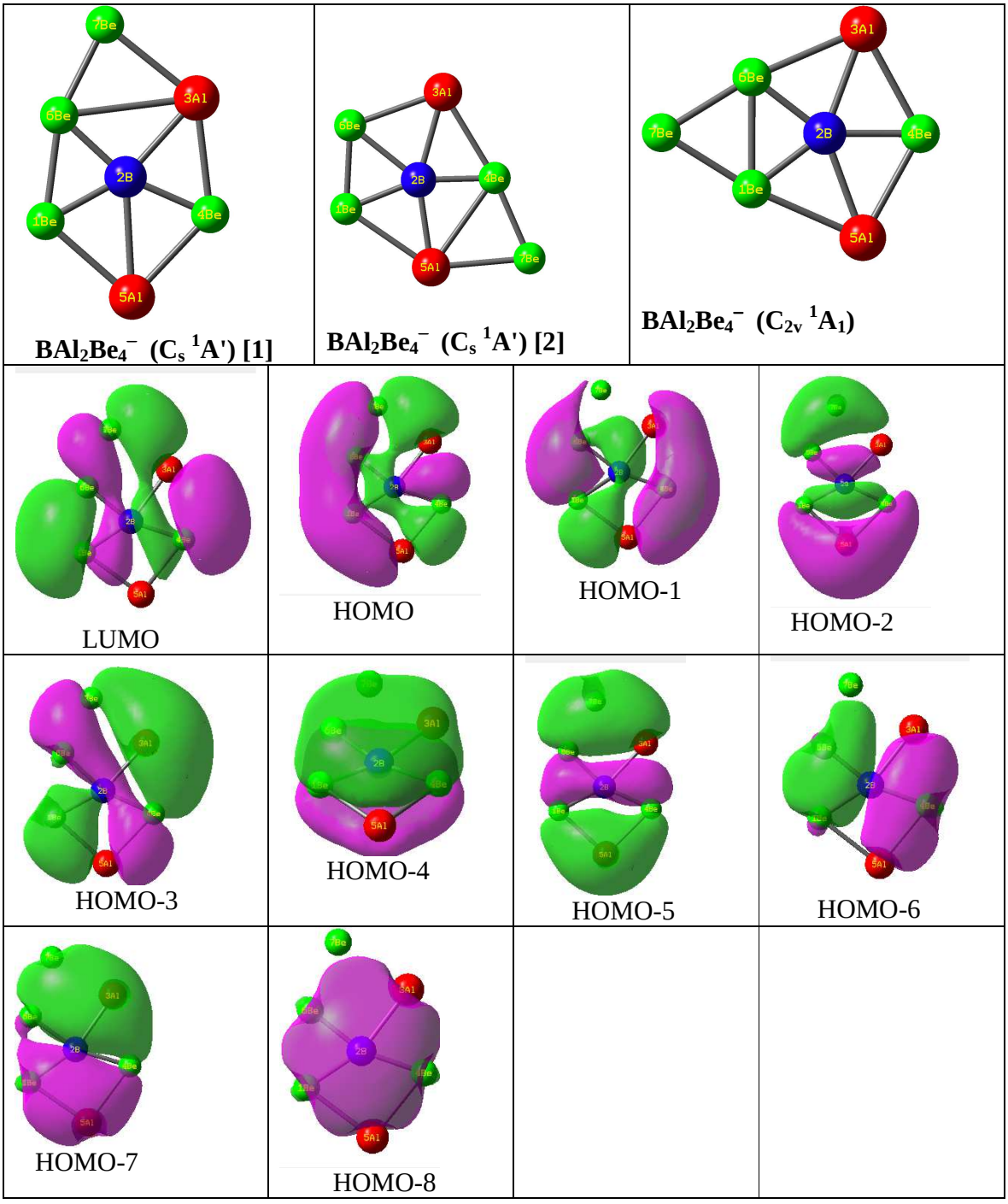

Fig. S9. The optimized geometries of $BAl_2Be_4^-$ and the lowest unoccupied molecular orbital as well as all occupied valence molecular orbitals of $BAl_2Be_4^-$ (C_s $^1A'$) [1] at B3LYP/6-311+G(d) level.

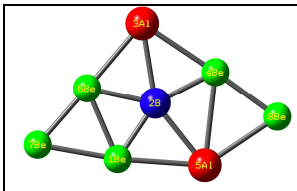

$BAl_2Be_5^+$ (C_s $^1A'$) [1] (NIMAG=0)

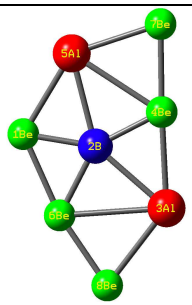

$BAl_2Be_5^+$ (C_s $^1A'$) [2] (NIMAG=0)

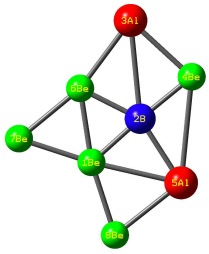

$BAl_2Be_5^+$ (C_s $^1A'$) [3] (NIMAG=1)

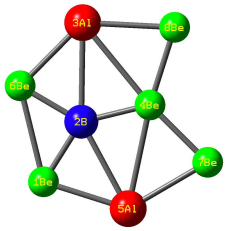

$BAl_2Be_5^+$ (C_s $^1A'$) [4] (NIMAG=1)

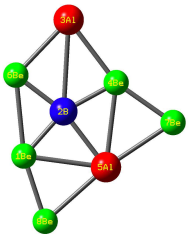

$BAl_2Be_5^+$ (C_s $^1A'$) [5] (NIMAG=1)

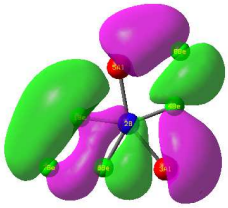

LUMO

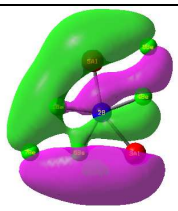

HOMO

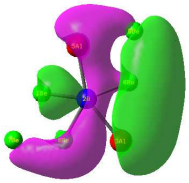

HOMO-1

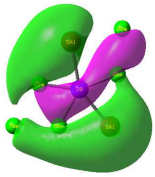

HOMO-2

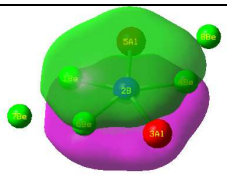

HOMO-3

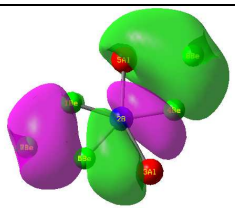

HOMO-4

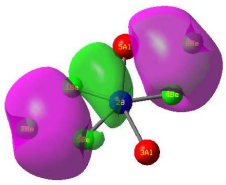

HOMO-5

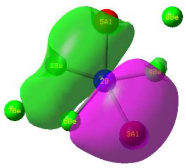

HOMO-6

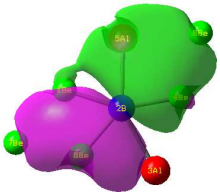

HOMO-7

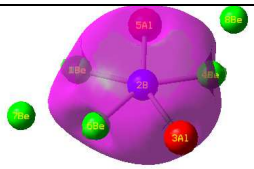

HOMO-8

Fig. S10. The optimized geometries of $BAl_2Be_5^+$ and the lowest unoccupied molecular orbital as well as all occupied valence molecular orbitals of $BAl_2Be_5^+$ (C_s $^1A'$) [1] at B3LYP/6-311+G(d) level.

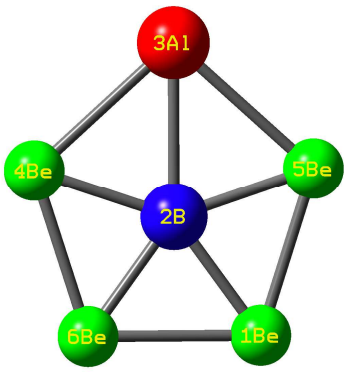

$BAlBe_4^{4-}$ (C_{2v} $^1A_1$)

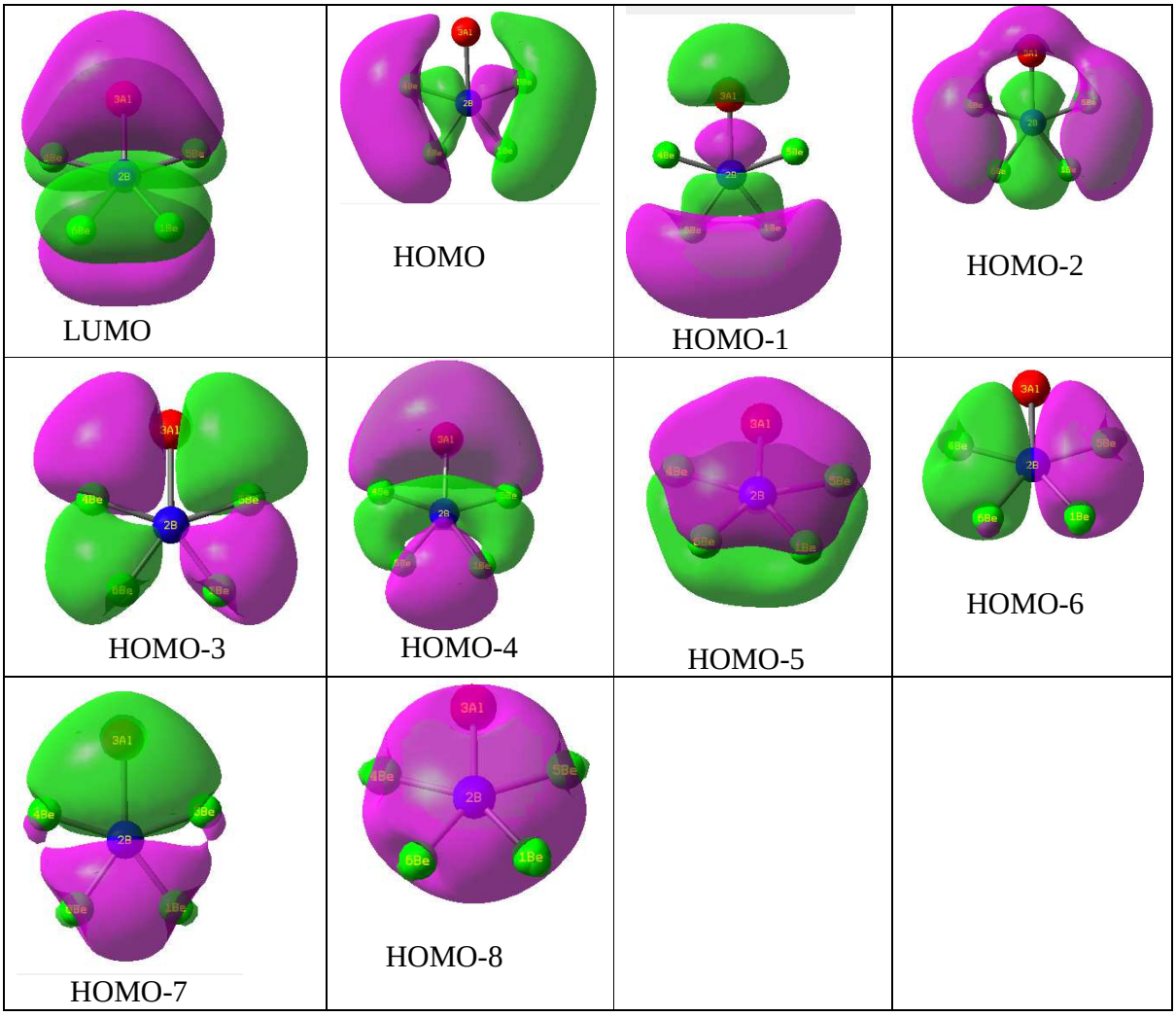

Fig. S11. The optimized geometries of $BAlBe_4^{4-}$ (C_{2v} $^1A_1$) and its lowest unoccupied molecular orbital as well as all occupied valence molecular orbitals at B3LYP/6-311+G(d) level.

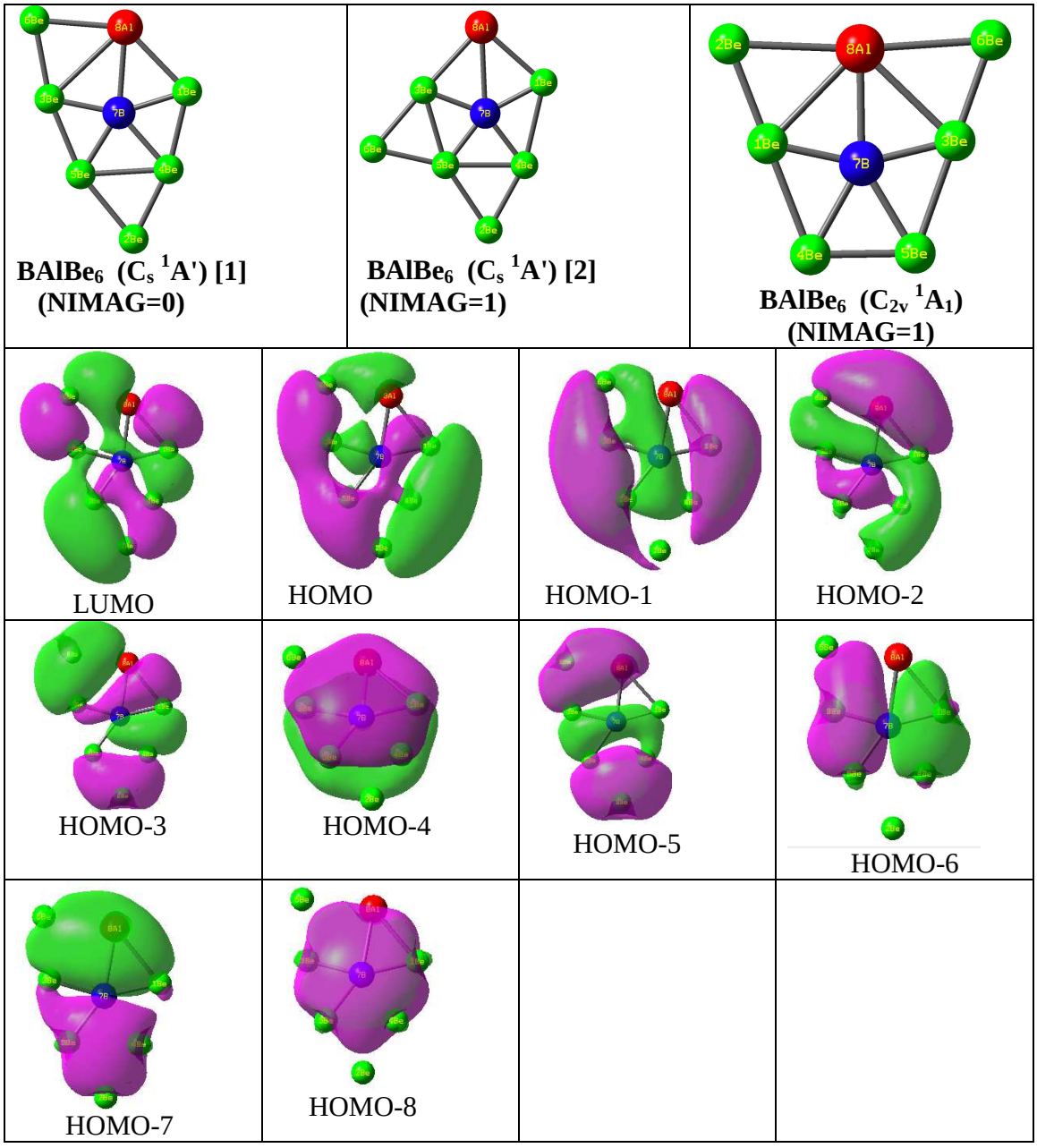

Fig. S12. The optimized geometries of $BAlBe_6$ and the lowest unoccupied molecular orbital as well as all occupied valence molecular orbitals of $BAlBe_6$ (C_s $^1A'$) [1] at B3LYP/6-311+G(d) level.

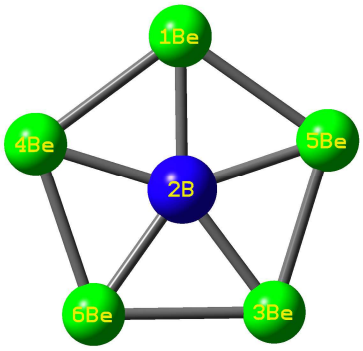

BBe_5^{5-} (D_{5h} $^1A_1'$)

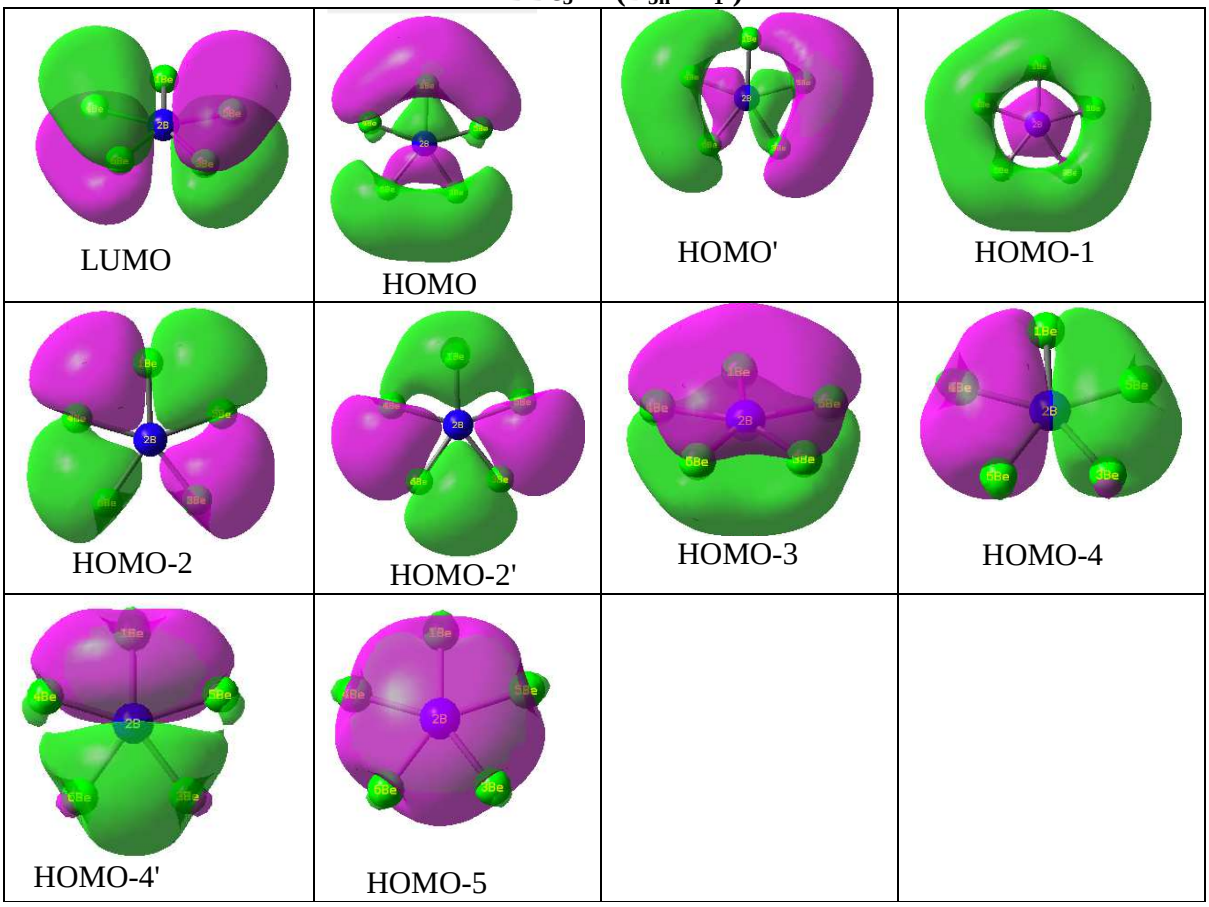

Fig. S13. The optimized geometries of BBe_5^{5-} (D_{5h} $^1A_1'$) and its lowest unoccupied molecular orbital as well as all occupied valence molecular orbitals at B3LYP/6-311+G(d) level.

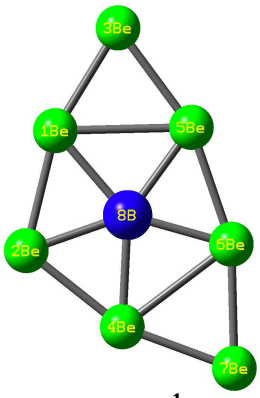

BBe_7^- (C_{2v} $^1A_1$) [1]
NIMAG=0

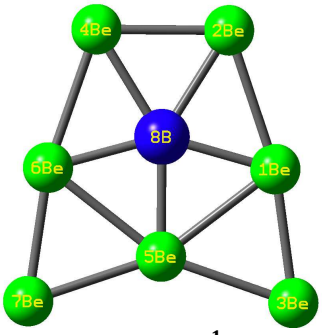

BBe_7^- (C_{2v} $^1A_1$) [2]
NIMAG=1

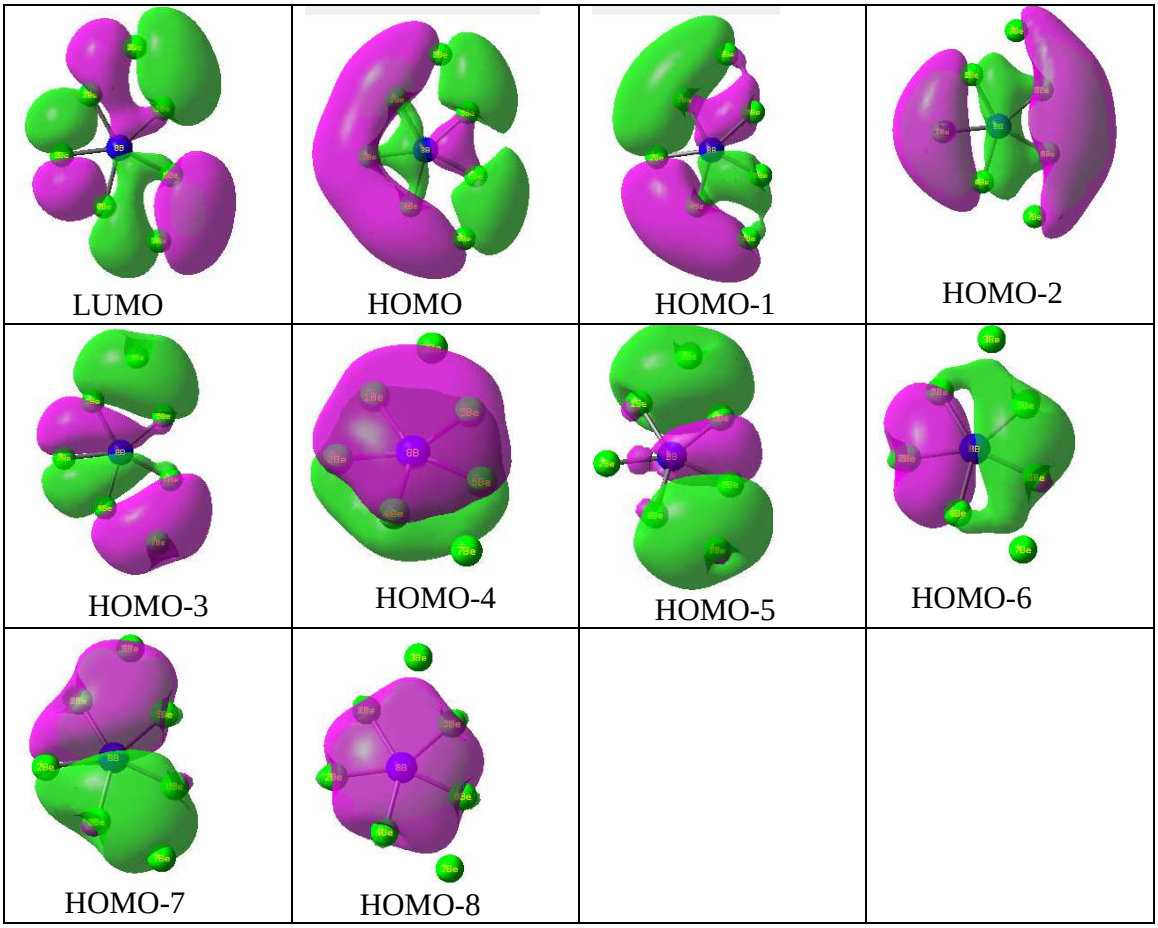

Fig. S14. The optimized geometries of BBe_7^- and the lowest unoccupied molecular orbital as well as all occupied valence molecular orbitals of BBe_7^- (C_{2v} $^1A_1$) [1] at B3LYP/6-311+G(d) level.

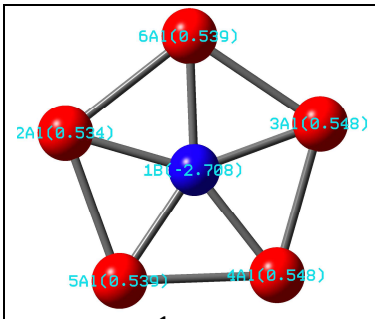

BAl_5 (D_{5h} $^1A_1'$)

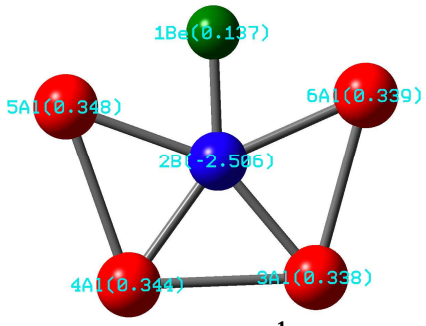

BAl_4Be^- (C_{2V} $^1A_1$)

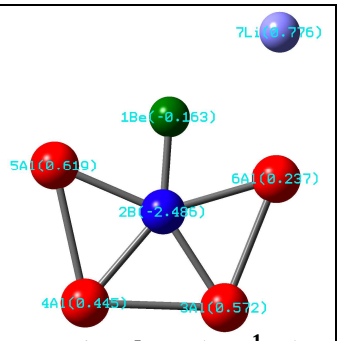

$LiBAl_4Be$ (C_s $^1A'$)

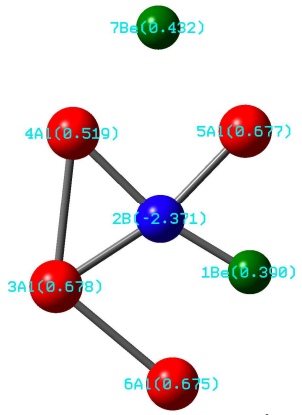

$BAl_4Be_2^+$ (C_s $^1A'$)

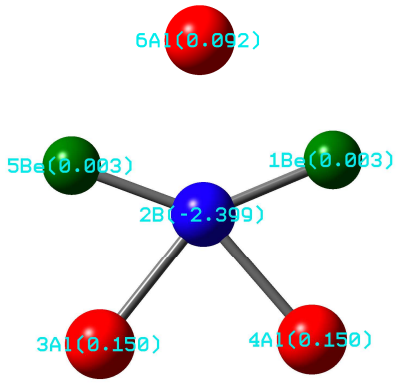

$BAl_3Be_2^{2-}$ (C_{2v} $^1A_1$)

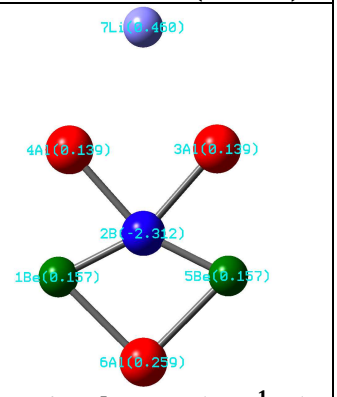

$LiBAl_3Be_2^-$ (C_{2v} $^1A_1$)

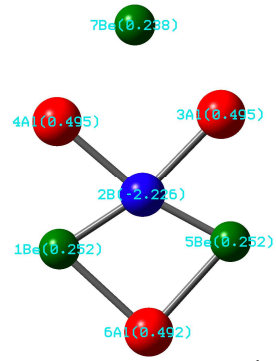

BAl_3Be_3 (C_{2v} $^1A_1$)

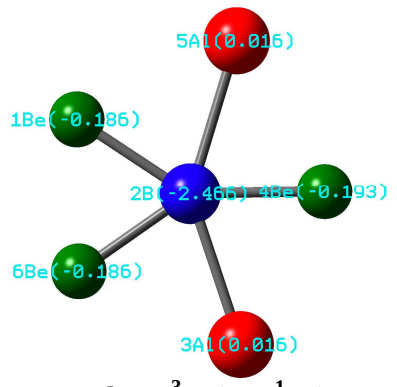

$BAl_2Be_3^{3-}$ (C_{2v} $^1A_1$)

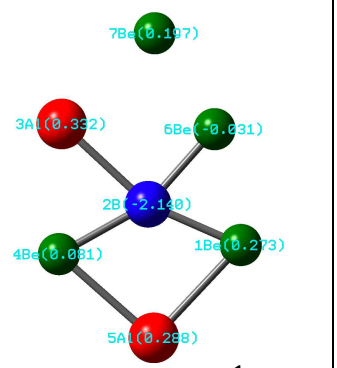

$BAl_2Be_4^-$ (C_s $^1A'$)

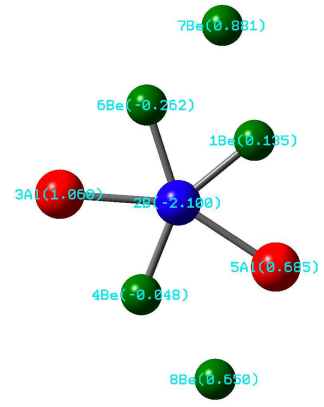

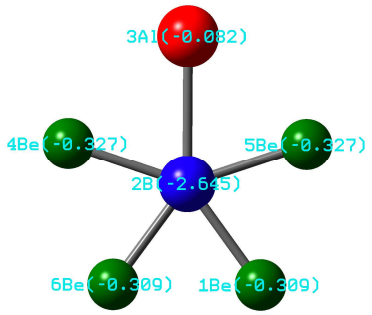

$BAlBe_4^{4-}$ (C_{2v} $^1A_1$)

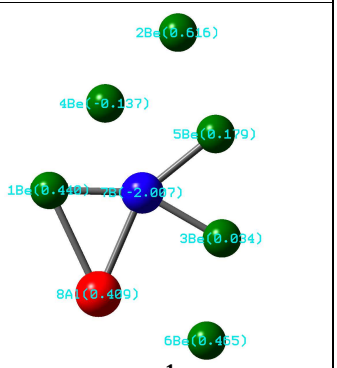

$BAlBe_6$ (C_s $^1A'$)

$BAl_2Be_5^+$ (C_s $^1A'$)		
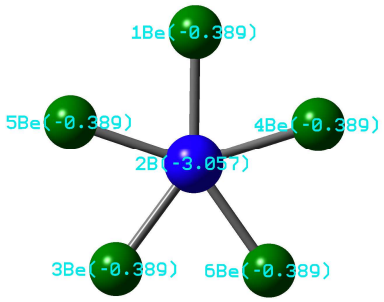 BBe_5^{5-} (D_{5h} $^1A_1'$)	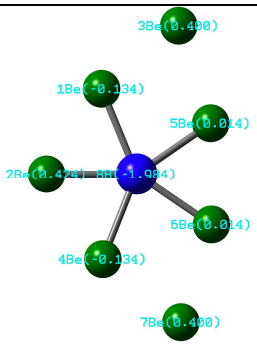 BBe_7^- (C_{2v} $^1A_1$)	

Fig. S15. The NPA charges on each atom calculated for the studied clusters at B3LYP/6-311+G(d) level.

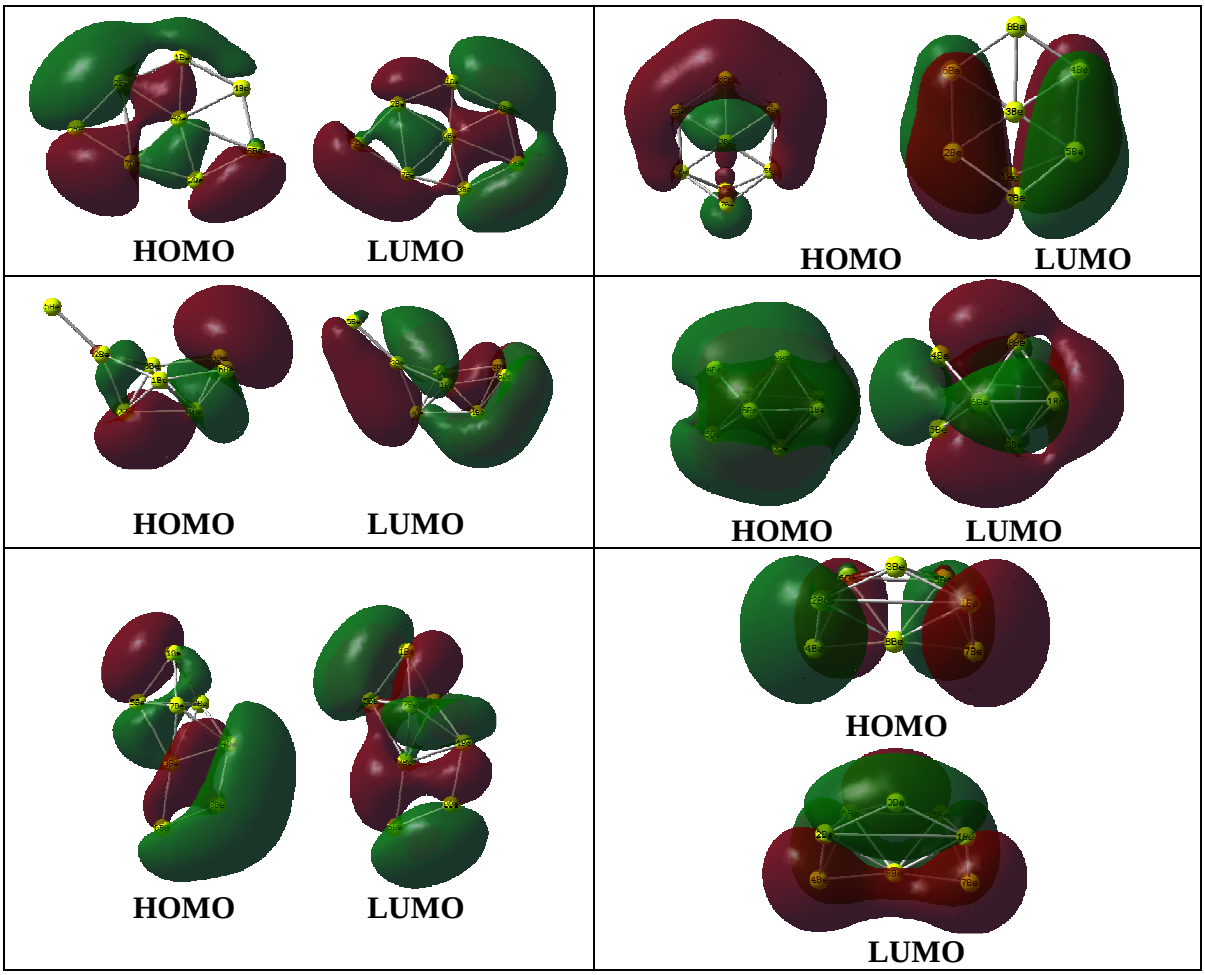

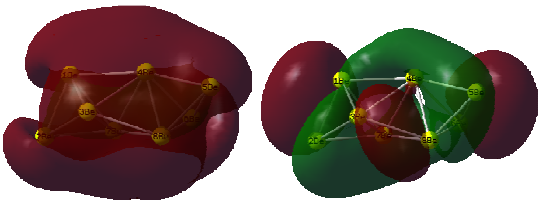

HOMO LUMO

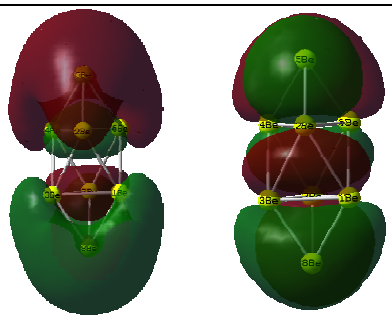

HOMO LUMO

HOMO LUMO

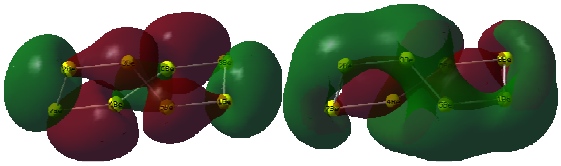

HOMO LUMO

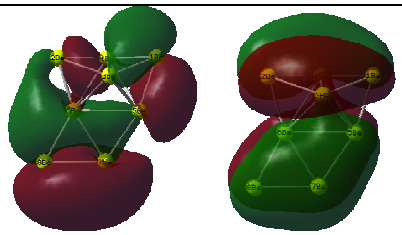

HOMO LUMO

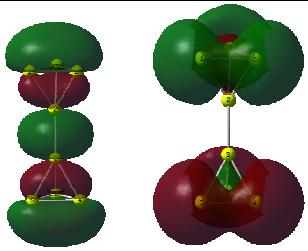

HOMO LUMO

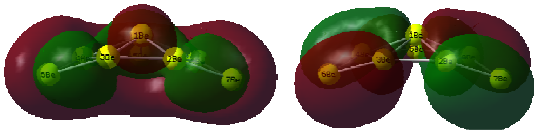

HOMO LUMO

HOMO

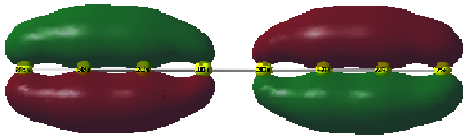

LUMO

Fig. S16: The frontier molecular orbital pictures of all the possible isomers of Be_8^{2-} molecule at B3LYP/6-311+G(d) level.